Title:

Isolation of a natural DNA virus of *Drosophila melanogaster*, and characterisation of host resistance and immune responses

Running title:

Isolation and characterisation of a DNA virus of *D. melanogaster*

Authors:

William H. Palmer *[1]
Nathan Medd [1]
Philippa M. Beard [3,4]
Darren J. Obbard [1,2]

Contact:

[1] Institute of Evolutionary Biology University of Edinburgh, Charlotte Auerbach Road, Edinburgh, UK
[2] Centre for Infection, Evolution and Immunity, University of Edinburgh, Charlotte Auerbach Road, Edinburgh, UK
3 The Roslin Institute and The Royal (Dick) School of Veterinary Studies, University of Edinburgh, EH25 9RG
4 Current Address: The Pirbright Institute, Ash Rd, Surrey, GU24 0NF

*Author for correspondence

Abstract

Drosophila melanogaster has played a key role in our understanding of invertebrate immunity. However, both functional and evolutionary studies of host-virus interaction in this model have been limited by a dearth of native *Drosophila* virus isolates. In particular, despite a long history of virus research, DNA viruses of *D. melanogaster* have only recently been described, and none have been available for experimental study. Here, we report the isolation and comprehensive characterisation of Kallithea virus, a large double-stranded DNA virus, and the first DNA virus to have been reported from wild populations of *D. melanogaster*. We find that Kallithea virus infection is costly for adult flies, reaching high titres in both sexes and reducing survival in males, and movement and late fecundity in females. Using the *Drosophila* Genetic Reference Panel we quantify host genetic variance for virus-induced mortality and viral titre, and identify candidate host genes that may underlie this variation, including *Cdc42-interacting protein 4*. Using full transcriptome sequencing of infected males and females, we examine the transcriptional response of flies to Kallithea virus infection, and find differential regulation of male-biased genes, and genes involved in innate immune pathways, cuticle development, chorion production, and serine endopeptidase activity. This work establishes Kallithea Virus as a new tractable model to study the natural relationship between *D. melanogaster* and DNA viruses, and we hope it will serve as a basis for future studies of immune responses to DNA viruses in insects.

Introduction

Studies of *Drosophila melanogaster* are central to our understanding of infection and immunity in insects. Moreover, many components of the *Drosophila* immune response, including parts of the JAK-STAT, IMD, and Toll (and perhaps RNA interference; RNAi) pathways are conserved from flies to mammals (Dupuis et al, 2003; Karst et al, 2003; Sharma et al, 2003; Zambon et al, 2005; Dostert et al, 2005; Wang et al, 2006; Avadhanula et al, 2009; Maillard et al, 2013; Li et al, 2013), making *Drosophila* a valuable model beyond the insects. The experimental dissection of antiviral immune pathways in *Drosophila* has benefited from both natural infectious agents of *Drosophila*, such as Drosophila C Virus (DCV) and Sigma virus (DmelSV), and from artificial infections, such as Cricket paralysis virus (isolated from a cricket), Flock House Virus (from a beetle), Sindbis virus (from a mosquito) and Invertebrate Iridescent Virus 6 (from a moth). However, while the availability of experimentally tractable, but non-natural, model viruses has been a boon to studies of infection, it also has two potential disadvantages. First, the coevolutionary process means that pairs of hosts and pathogens which share a history may

interact very differently to naive pairs (e.g. Ferguson and Read, 2002; Compton et al, 2012). For example, the Nora virus of *D. immigrans* expresses a viral suppressor of RNAi that is functional in the natural host, but not in *D. melanogaster* (van Mierlo et al, 2014). Second, if our aim is to understand the coevolutionary process itself, then the standing diversity in both host and virus populations may be fundamentally altered in coevolving as opposed to naïve pairs. For example, heritable variation for host resistance was detectable for two natural viruses of *D. melanogaster*, but not for two non-natural viruses (Magwire et al, 2012; Wang et al, 2017). This difference was in part due to large-effect segregating polymorphisms for resistance to the natural viruses, which are predicted to result from active coevolutionary dynamics (Contamine et al, 1989; Magwire et al, 2011; Magwire et al, 2012; Cogni et al, 2017).

Experimental studies of host-virus interaction using *Drosophila* have consequently been limited by a lack of diverse natural virus isolates. In particular, no natural DNA viral pathogens of *D. melanogaster* have previously been isolated (Brun and Plus, 1980; Huszar and Imler, 2008; but see Unckless, 2011 for a DNA virus of *Drosophila innubila*), and all natural (and most artificial) studies of viral infection in *D. melanogaster* have therefore focussed on the biology of RNA viruses and antiviral resistance (Xu and Cherry, 2014; Bronckhorst et al, 2012). For DNA viruses, our molecular understanding of insect-virus interaction has instead largely been shaped by the response of lepidopterans to their natural Baculoviruses, which are often of agronomic and/or ecological importance (Herniou et al, 2004), but lack the genetic toolkit of *D. melanogaster*. Nevertheless, Lepidopteran expression studies in response to baculovirus infection have implicated host genes with a diverse array of functions, including cuticle proteins, reverse transcriptases, and apoptotic factors, suggesting previously uncharacterised and/or host-specific antiviral immune mechanisms (Breitenbach et al, 2011; Noland et al, 2013; Nguyen et al, 2013; McTaggart et al 2015).

The only DNA virus studies to date in *D. melanogaster* have used Insect Iridescent Virus 6 (IIV6), an enveloped dsDNA moth iridovirus with an extremely broad host range (Williams 2008). This work has shown that *Drosophila* RNAi mutants are hyper-susceptible to IIV6 infection, and that IIV6 encodes a viral suppressor of RNAi, indicating that at least some immune responses to DNA viruses overlap substantially with those to RNA viruses (Kemp et al, 2012; Bronkhorst et al, 2012; Bronkhorst et al, 2014). However, while IIV6 injections are lethal in *D. melanogaster*, and IIV6 has provided useful information about the *Drosophila* response to DNA viruses, for the reasons described above, it is hard to interpret the implications of this for our understanding of natural host-virus interaction.

Metagenomic sequencing has identified natural dsDNA Nudivirus infections in wild-caught *D. innubila* (*D. innubila* Nudivirus, DiNV; Unckless, 2011; Hill and Unckless, 2017) and in *D. melanogaster* and *D. simulans* ('Kallithea virus', KV; Webster et al, 2015; 'Esparto virus' and 'Tomelloso virus'; DrosEU Consortium unpublished data), and also ssDNA Densovirus infections in *D. melanogaster* and *D. simulans* ('Vesanto virus', 'Linvill Road virus', and 'Viltain virus', DrosEU Consortium unpublished data). Like other members of the Nudiviridae, DiNV and KV are enveloped dsDNA viruses of around 120-230Kbp with 100-150 genes. This recently-recognised family forms a clade that is either sister to, or paraphyletic with, the Bracoviruses (Thézé et al, 2011), which have been 'domesticated' by Braconid parasitoid wasps following genomic integration, and now provide key components of the wasp venom (Herniou et al, 2013; Gauthier et al, 2017). Together, the nudiviruses and bracoviruses are sister to the baculoviruses, arguably the best-studied dsDNA viruses of insects. They share many of their core genes with baculoviruses, but canonically lack occlusion bodies (Wang and Jehle, 2009). PCR surveys of wild flies suggest that DiNV is common in several species in the subgenus *Drosophila*, and that KV is widespread and common in *D. melanogaster* and *D. simulans*, being detectable in 10 of 17 tested populations, with an estimated global prevalence of 2-7% (Webster et al, 2015). However, we currently know little about the interaction between these viruses and their hosts. Indeed, although studies of wild-caught *D. innubila* individuals infected by DiNV suggest that infection is costly (Unckless 2011), in the absence of an experimental *D. melanogaster* Nudivirus isolate, it has not been possible to capitalise the power of *D. melanogaster* genetics to further elucidate the costs associated with infection, or the genetic basis of resistance.

Here we present the isolation of KV from wild-collected *D. melanogaster* via passage in laboratory stocks and gradient centrifugation. We use this isolate to characterise the fundamental phenotypic impacts of infection on host longevity and fecundity. We then use the *Drosophila* Genetic Reference Panel (DGRP) to quantify and dissect genetic variation in immunity to KV infection in males and females, and we use RNAseq analyses of an inbred line to quantify host and virus transcriptional response in both sexes. We find that KV causes higher rates of mortality following injection in males, but that male and female viral titres do not differ substantially, suggesting some female tolerance to infection. However, we also find that female movement is decreased following infection, and that infected females have significantly reduced late-life fecundity—highlighting the importance of considering infection phenotypes beyond longevity. We find a genetic correlation in longevity between KV-infected males and

females, and a weak negative genetic correlation between mortality and KV titre in females, and we report host loci that have variants significantly associated with each trait. Finally, our expression analysis of infected individuals suggests a dramatic cessation of oogenesis following infection, and significant differential regulation of serine proteases, cuticle proteins, and certain immune genes. This work establishes KV as a new natural model for DNA virus infection in *D. melanogaster*, and will enable further dissection of the insect antiviral immune response.

Materials and Methods

Isolation of Kallithea Virus

We identified KV-infected flies through a PCR screen for previously published *D. melanogaster* viruses in 80 previously un-tested wild-caught flies (see Webster et al, 2015 for primers and cycling conditions). We homogenised each fly in 0.1 mL of Ringer's solution, transferred half of the homogenate to Trizol for nucleic acid extraction, and performed RT PCR assays on the resulting RNA for all *D. melanogaster* viruses reported by Webster *et al* (2015). We selected a KV-positive sample from Thika, Kenya (Collected by John Pool in 2009; subsequently stored at -80C), removed debris from the remaining fly homogenate by centrifugation for 10 minutes at 1000 × g, and microinjected 50 nL of the supernatant into *Dicer-2*^{L811fsX} flies, which lack a robust antiviral immune response (Lee et al, 2004). After one week, we homogenised 100 KV-injected *Dicer-2* ^{L811fsX} flies in 10 uL Ringer's solution per fly, cleared the solution by centrifugation as above, and re-injected this homogenate into further *Dicer-2*^{L811fsX} flies. This process was then repeated twice more with the aim of increasing viral titres. In the final round of serial passage, we injected 2000 *Dicer-2* ^{L811fsX} flies, which were homogenised in 5 mL 10 mM Tris-HCl. We cleared the homogenate by centrifuging at 1000 × g for 10 minutes, filtering through cheese cloth, centrifuging twice more at 6000 × g for 10 minutes, and finally filtering through a Millex 0.45 µm polyvinylidene fluoride syringe filter. The resulting crude virus preparation was used as input for gradient ultracentrifugation.

We screened the crude preparation by RT-PCR for other published *Drosophila* virus sequences, and identified the presence of DAV, Nora virus, DCV, and La Jolla virus. To separate KV from these viruses, we used equilibrium buoyant density centrifugation in iodixanol ("OptiPrep", Sigma-Aldrich) as enveloped viruses are expected to have lower buoyant densities than most unenveloped viruses. Iodixanol is biologically inert, and gradient fractions can be used directly for downstream infection experiments (avoiding dialysis, which we found greatly reduces KV titres). We concentrated virus particles by centrifuging crude virus solution through a 1 mL

10% iodixanol layer onto a 2 mL 30% iodixanol cushion at 230,000 × g for 4 hours in a Beckman SW40 rotor. Virus particles were taken from the 30%-10% interphase, and layered onto a 40%-10% iodixanol step gradient, with 2% step changes, and centrifuged for 48 hours at 160,000 × g. We fractionated the gradient at 0.5 mL intervals, phenol-chloroform extracted total nucleic acid from aliquots of each fraction, and measured virus concentration by quantitative PCR (qPCR). We pooled all Kallithea-positive, RNA virus-negative fractions and calculated the infectious dose 50 (ID50) by injecting 3 vials of 10 flies with a series of 10-fold dilutions and performing qPCR after 5 days. We also performed the above isolation protocol with uninfected *Dicer-2*^{L811fsX} flies, and extracted the equivalent fractions for use as an injection control solution (hereafter referred to as "gradient control").

Transmission electron microscopy

A droplet of viral suspension was allowed to settle on a Formvar/Carbon 200 mesh Copper grid for 10 minutes. We removed excess solution, and applied a drop of 1% aqueous uranyl acetate for 1 minute before removing the excess by touching the grid edge with filter paper. The grids were then air dried. Samples were viewed using a JEOL JEM-1400 Plus transmission electron microscope, and representative images were collected on a GATAN OneView camera.

Measurement and analysis of viral titre

Flies were reared on a standard cornmeal diet until infection, after which they were transferred to a solid sucrose-agar medium. We infected flies by abdominal injection of 50 nL of 10^5 ID50 KV using a Nanoject II (Drummond Scientific), and these flies were then used to assay changes in viral titre, mortality, fecundity, or daily movement. To test whether viral titre over time was influenced by sex or the presence of *Wolbachia* endosymbionts, we injected 25 vials of 10 male or female *Oregon R* flies with KV, with or without *Wolbachia* (totalling 1000 flies). We phenol-chloroform extracted total nucleic acid at 5 time points: directly after injection and 3, 5, 10, and 15 days post-infection. We used qPCR to measure viral titre relative to copies of the fly genome with the following (PCR primers: kallithea_126072F CATCAATATCGCGCCATGCC, kallithea_126177R GACCGAGTTAGCGTCAATGC, rpl32_465F CTAAGCTGTCGGTGAGTGCC, rpl32_571R: TGTTGTCGATACCCTTGGGC). We analysed the log-transformed relative expression levels of Kallithea virus as a Gaussian response variable in a linear mixed model using the Bayesian generalised mixed modelling R package MCMCglmm (V2.24; Hadfield, 2010, see supporting text for code to fit all models).

The model took the form

$$y_{ijkl}^{titre} = \beta_0 + \beta_j^{DPI} + \beta_k^{sex} + \beta_{jk}^{DPI:sex} + \mu_l^{plate} + \varepsilon_{ijkl} \qquad [1]$$

where y_{ijkl}^{titre} is the log-transformed viral titre relative to fly genomic copies in the i^{th} vial of flies j days after infection, with sex (k), as measured on qPCR plate l. The fixed effects portion of the model included an intercept term (β_0) and coefficients for the number of days post-infection (DPI; β^{DPI}), sex (β^{sex}), and DPI by sex interaction ($\beta^{DPI:sex}$). We estimated random effects for the l^{th} qPCR plate as μ^{plate} and the residuals as ε_{ijkl}, and assumed both are normally distributed. We initially fitted the model with *Wolbachia* infection status included as a fixed effect, however this term was not significant and was excluded from the final model.

We also attempted to infect flies with KV by feeding. We anesthetised flies in an agar vial, and sprayed 50 uL of $5x10^3$ ID50 KV onto the flies and food. We then collected flies immediately (for the zero time-point) and at 7 DPI, and used the primers above to calculate relative KV titre.

Mortality following KV infection

We performed mortality assays to test the effect of KV infection on longevity, and to test whether this was affected by sex or *Wolbachia* infection status. We injected a total of 1200 *Oregon R* flies with control gradient or KV for each sex with or without *Wolbachia* (*Wolbachia* had previously been cleared by 3 generations of Ampicillin treatment, and was confirmed by PCR). We maintained flies of each treatment in 10 vials of 10 flies, and recorded mortality daily for three weeks. Mortality that occurred in the first day after infection was assumed to be due to the injection procedure and excluded from further analysis. We analysed mortality using an event-analysis framework as a generalised linear mixed model in MCMCglmm, with per-day mortality in each vial as a binomial response variable,

$$y_{ijkm}^{alive}, y_{ijkm}^{dead} = logit^{-1}(\beta_0 + \beta_j^{DPI} + \beta_j^{DPI^2} + \beta_k^{sex} + \beta_m^{KV} + \beta_{jk}^{DPI:sex} + \beta_{jm}^{DPI:KV} + \beta_{jkm}^{DPI:KV:sex} + \mu_i^{vial} + \varepsilon_{ijkm}) \qquad [2]$$

where y_{ijkm}^{alive} and y_{ijkm}^{dead} are the number of flies alive and dead in the i^{th} vial on the j^{th} day. In addition to the fixed effects in equation [1], we also included a quadratic term to capture non-linear mortality curves (β^{DPI^2}), an effect for the difference between KV-infected versus control-injected flies (β^{KV}), and interactions between KV infection status and the other fixed effect variables ($\beta^{DPI:KV}$, $\beta^{DPI:KV:sex}$). We fitted random effects for each vial (μ^{vial}) to account for non-independence among flies within vials, assuming these follow a normal distribution. As in

the model for viral titre, we found no evidence for differences associated with *Wolbachia* infection, and *Wolbachia* terms were excluded from the final model. The higher rate of male mortality we observed was also confirmed in a second independent experiment using an outbred population derived from the Drosophila Genetic Reference Panel (DGRP; see below).

Fecundity following KV infection

We measured fecundity for 12 days following infection. Virgin female flies from an outbred population derived from the DGRP were injected with either KV, or with chloroform-inactivated KV as a control, and individually transferred to standard cornmeal vials. The following day, we introduced a single male fly into the vial with the virgin female. We transferred the pair to new vials each day, and recorded the number of eggs laid. Per-day fecundity was analysed in MCMCglmm as a Poisson response variable (y_{ijm}^{egg}) using a hurdle model, which models the probability of zeroes (y_{ijm}^{zero}) in the data and the Poisson process as separate variables. The model took the form,

$$y_{ijm}^{egg}, y_{ijm}^{zero} = \exp(\beta_0 + \beta_j^{DPI} + \beta_m^{KV} + \beta_{jm}^{DPI:KV} + \mu_i^{vial} + \varepsilon_{ijm}) \qquad [3]$$

with fixed effects associated with KV infection status, DPI, and the interaction between KV infection and DPI, and random effects associated with each fly pair (vial). The analysis was performed with DPI coded as either a continuous or categorical variable (to test for per-day differences), and results were qualitatively similar.

We analysed ovary morphology to confirm egg production was halted. Flies were injected with either control virus solution or KV and kept on agar vials. After 8 DPI, flies were transferred to vials with lewis medium supplemented with yeast. Two days later, we dissected ovaries in phosphate-buffered saline solution, fixed ovaries in 4% paraformaldehyde, and stained nuclei with DAPI. Ovaries were analysed under a Leica fluorescence microscope, and we recorded whether each ovariole within an ovary included egg chambers past stage 8 (i.e. had begun vitellogenesis), and whether any egg chambers within an ovariole exhibited apoptotic nurse cells. Each of these traits were analysed using a logistic regression in MCMCglmm,

$$p_{im}^{mature} = logit^{-1}(\beta_0 + \beta_m^{KV} + \mu_i^{ovary} + \varepsilon_{im}) \qquad [4]$$

where p_{im}^{mature} is the probability of an ovariole containing a post-vitellogenic egg chamber, and μ^{ovary} is a random effect associated with each ovary that an ovariole is derived. We analysed whether apoptotic nurse cells are associated with KV virus-infected ovary in a similar manner.

Daily movement following KV infection

We used a *Drosophila* Activity Monitor (DAM, TriKinetics; Pfeiffenberger et al, 2010) to measure per-day total movement of individual flies (Pfeiffenberger et al, 2010). The DAM is composed of multiple hubs, each with 32 tubes containing a single fly, and movement is recorded on each occasion the fly breaks a light beam. We injected 96 female flies from an outbred DGRP population (created from 113 DGRP lines and maintained at a low larval density with non-overlapping generations) with either chloroform-inactivated KV or KV, randomly assigned these flies within and across 3 hubs, and measured total movement for one week. Movement was binned for each day and this per-day total movement ($y_{ijmn}^{movement}$) was analysed in a linear mixed model using MCMCglmm as a Poisson response variable:

$$y_{ijmn}^{movement} = \exp(\beta_0 + \beta_j^{DPI} + \beta_m^{KV} + \beta_{jm}^{DPI:KV} + \mu_i^{fly} + \mu_n^{hub} + \varepsilon_{ijmn}) \quad [5]$$

We completely excluded flies that failed to move for a whole day or longer, assuming them to be dead. As before, we included fixed effects associated with DPI, KV infection status, and the interaction between KV and DPI. We included random effects associated with each of the i flies (repeated measures) and each of n hubs (μ^{hub}), and assumed each of these take values from a normal distribution.

Quantitative genetic analysis

The DGRP is a collection of highly inbred fly lines derived from a *D. melanogaster* population collected in Raleigh, North Carolina (Mackay et al, 2012), and is widely used to estimate and dissect genetic variation in complex traits in *Drosophila*. We measured KV titre in females and mortality following KV infection in both sexes for 125 DGRP lines, and estimated genetic (line) variances and covariances among these traits. To measure viral titre in the DGRP, we infected 5 vials of 10 flies for each line across 5 days, with a vial from each line being represented each day. After 8 DPI, living flies were killed and homogenised in Trizol for nucleic acid extraction and qPCR. To measure mortality following KV infection in the DGRP, we injected 3 vials of 10 flies of each sex and recorded mortality on alternate days until half the flies in the vial were dead (i.e. median survival time). Flies were transferred to fresh agar vials every 10 days. Mortality occurring in the first 3 DPI was assumed to be caused by the injection procedure, and was removed from the analysis.

We fitted a multi-response linear mixed model in MCMCglmm to estimate heritability and genetic covariances among lines

$$y_{iklpqr}^{trait} = \beta_p^{trait} + \beta_{pk}^{trait:sex} + \mu_{pq}^{trait:date} + \mu_l^{plate} + \mu_{pkr}^{trait:sex:line} + \varepsilon_{iklpqr}^{trait:sex} \quad [6]$$

where y_{iklpqr}^{trait} is the log-transformed relative viral titre or the duration until median mortality (LT50). We only estimated sex-specific fixed effects ($\beta^{trait:sex}$) for LT50, because we did not

measure titre in both sexes. The first part of the random effects model accounts for block effects due to date of injection ($\mu^{trait:date}$) and qPCR plate (μ^{plate}). We assumed a 2x2 identity matrix as the covariance structure for $\mu^{trait:date}$, with effects associated with each trait from independent normal distributions. Effects for the l^{th} plate were assumed to be normally distributed. The second part of the random effects model ($\mu^{trait:sex:line}$) estimates the variance in each trait across lines, and is allowed to vary by sex. We estimated all variance-covariance components of the 3x3 G matrix associated with $\mu^{trait:sex:line}$. Finally, we fitted separate error variances for each trait in each sex ($\varepsilon^{trait:sex}$), where residuals are associated with independent normal distributions.

The diagonal elements of the $\mu^{trait:sex:line}$ covariance matrix represent posterior distributions of genetic variances for viral titre in females, LT50 in females, and LT50 in males (V_G^{titre}, $V_G^{mortality♀}$, $V_G^{mortality♂}$). We calculated broad-sense heritability (i.e. line effects) for each trait as $H^2 = \frac{V_G}{V_G+V_R}$, where V_R is the residual variance associated with each trait, estimated in the model as $\varepsilon^{trait:sex}$. However, heritabilities cannot readily be compared because of their dependence on the residual variance, which can be vastly different for different phenotypes (Houle, 1992). Therefore, we also calculate the coefficient of genetic variation (CV_G) as $CV_G = \frac{100*\sqrt{V_G}}{\mu}$, where V_G is standardised by the phenotypic mean (μ), and is more appropriate for comparisons across phenotypes. All confidence intervals reported are 95% highest posterior density intervals.

Genome-wide association studies

We used measurements of viral titre and mortality following KV infection in the DGRP lines to perform a series of genome-wide association studies (GWAS). Although our power to detect small-effect genetic variants with only 125 lines is very low, past studies have demonstrated genetic variation in natural viral resistance in *Drosophila* is often dominated by few large effect variants (Contamine et al, 1989; Magwire et al, 2011; Magwire et al, 2012; Cogni et al, 2017; but see King and Long, 2017). We performed a GWAS on each phenotype separately by fitting an individual linear model for each variant in the genome using the full data.

$$log\left(y_{ilqs}^{titre}\right) = \beta_0+\beta_s^{SNP}+\beta_l^{plate}+\beta_q^{date}+\varepsilon_{ilqs} \quad [7]$$

$$y_{iks}^{mortality} = \beta_0+\beta_k^{Sex}+\beta_s^{SNP}+\beta_{ks}^{Sex:SNP}+\varepsilon_{iks} \quad [8]$$

Models were fitted using the base R linear model function 'lm()'. We tested the significance of β^{SNP} and $\beta^{Sex:SNP}$ with a t-test, and we obtained significance thresholds for each GWAS by permuting genotypes across phenotypes 1000 times, and recording the lowest *p*-value for each pseudo-dataset. Code for this model is provided in Supplementary text 1.

Confirmation of GWAS hits

We chose 19 genes identified near significant GWAS hits to confirm their involvement in KV infection. For each gene, we crossed a transgenic line containing a homologous foldback hairpin under the control of the Upstream Activating Sequence (UAS) to two GAL4 lines: *w*; P{UAS-3xFLAG.dCas9.VPR}attP40, P{tubP-GAL80^{ts}}10; P{tubP-GAL4}LL7/TM6B, Tb^{1}* (Bloomington line #67065; hereafter referred to as *tub-GAL4*) and *w*; P{GawB}Myo31DF^{NP0001}/CyO; P{UAS-3xFLAG.dCas9.VPR}attP2, P{tubP-GAL80^{ts}}2* (Bloomington line #67067; hereafter referred to as *myo31DF-GAL4*). These lines drive GAL4 expression in the entire fly and in the gut, respectively, and contain a temperature-sensitive Gal80, which is able to inhibit GAL4 at the permissive temperature (18 degrees). RNAi lines included the following genes (BDSC numbers): *Pkcdelta* (28355), *btd* (29453), dos (31766), *tll* (34329), *Atg10* (40859), *Dgk* (41944), *Cip4* (53321), *hppy* (53884), *LpR2* (54461), *CG5002* (55359), *sev* (55866), *eya* (57314), *Gprk2* (57316), *Sox21b* (60120), *CG11570* (65014), *ATPCL* (65175), *Pdcd4* (66341), *CG7248* (67231), and *yin* (67334). As a control, we crossed the genetic background of the RNAi lines (Bloomington line #36304) to the two GAL4 lines. All crosses were made at 18 degrees. After eclosion, offspring were transferred to agar vials (10 flies per vial) at the non-permissive temperature (29 degrees) for two days to facilitate silencing of candidate genes, then injected with KV. We measured titre 5 DPI for 5 vials of each KV-infected genotype for each GAL4 driver. Results from each GAL4 line were analysed separately as in equation [1], except sex-specific effects were excluded, and we added a fixed effect for genotype. If the posterior distribution of the fixed effect associated with a candidate gene did not overlap zero, we concluded this gene is involved in KV infection.

Sample preparation for RNA-sequencing

We next aimed to characterise the host expression response to KV infection, and whether this differed between males and females. We injected 6 vials of 10 flies for each sex with either the control gradient solution or with KV. After 3 DPI, we homogenised flies in Trizol, extracted total nucleic acid, and enriched the sample for mRNA through DNAse treatment and poly-A selection. We used the NEB Next Ultra Directional RNA Library Prep Kit to make strand-

specific paired-end libraries for each sample, following manufacturer's instructions. Libraries were pooled and sequenced by Edinburgh Genomics using three lanes of an Illumina HiSeq 4000 platform with strand-specific 75 nucleotide paired end reads. All reads have been submitted to the European Nucleotide Archive under project accession ERP023609.

Differential expression analysis

We removed known sequence contaminants (primer and adapter sequences) from the paired end reads with cutadapt (V1.8.1; Martin, 2011) and mapped remaining reads to the *D. melanogaster* genome (FlyBase release r6.15) and to all known *Drosophila* virus genomes using STAR (V2.5.3a; Dobin et al, 2013), with a maximum intron size of 100 KB, but otherwise default settings. We counted the number of reads mapping to each gene using the featurecounts command in the subread package (V1.5.2; Liao et al, 2013) and used these raw count data as input to DESeq2 (V1.16.0; Love et al, 2014) for differential expression analysis. DESeq2 fits a generalised linear model for each gene, where read counts (K) are modelled as a negative binomially distributed variable (Anders and Huber, 2010; Love et al, 2014). Generally, the model takes the form

$$K \sim NB(s * log_2(X\beta), \alpha) \quad [9]$$

where s is a sample-specific size factor that controls for sequencing depth, $X\beta$ is the design matrix and associated linear predictors, and α is a dispersion parameter that depends on the shared variance of read counts for genes expressed at similar levels (Anders and Huber, 2010; Love et al, 2014). Our design matrix included sex, KV infection status, and the interaction between the two, allowing us to test for expression changes following KV infection and how these changes differ between the sexes. We calculated $\log_2$ fold changes in DESeq2, and tested for significance using Wald tests. We used the 'plotPCA' function implemented in DESeq2 to perform principal component analysis of the rlog-transformed read count data.

GO term analysis

We performed five independent gene ontology (GO) term enrichment analysis, using: (1) genes with significant SNPs in the GWAS for titre; (2) genes with significant SNPs in the GWAS for mortality, (3) genes upregulated in either sex ($p < 0.05$, log2 fold-change > 1); (4) genes downregulated in either sex ($p < 0.05$, log2 fold-change < -1); and (5), genes significantly different between males and females ($p < 0.05$, absolute log2 fold-change > 1). For each of these gene lists, we tested for GO term enrichment using the 'goseq' R package (V1.26.0; Young et al, 2010), which accounts for the difference in power for detecting differential expression caused by gene length, and tests for significant over-representation of genes in a GO

term.

Results and Discussion

Isolation of Kallithea Virus

We isolated Kallithea Virus (KV) by gradient centrifugation following 4 rounds of serial passage in flies. Many laboratory fly stocks and cell culture lines are persistently infected with RNA viruses (Brun and Plus, 1980; Webster et al, 2015), and following serial passage we identified co-infections of Drosophila A Virus (DAV), Nora Virus, and Drosophila C Virus (DCV) by PCR. The high prevalence of these viruses in laboratory stocks presents a substantial hurdle in the isolation of new *Drosophila* viruses, requiring the separation of the new viruses of interest. Although this can be relatively simple (e.g. separating enveloped from non-enveloped viruses), most of the recently identified *Drosophila* viruses (Webster et al, 2015; Webster et al, 2016; Medd et al, 2017) are from ssRNA virus families with buoyant densities similar to common laboratory infections. To exclude these from our isolate, we concentrated KV using a 1.18 g/mL cushion, retaining KV at the interphase, but excluding most of the contaminating RNA viruses. Subsequent equilibrium density gradient centrifugation produced a KV band at 1.17 g/mL, and with some DAV contamination at approximately 1.20 g/mL (Figure 1A). Although nudiviruses have not previously been prepared using an iodixanol gradient, the equilibrium buoyant density was consistent with the lower buoyant densities of enveloped particles (Feng et al, 2013) and similar to other enveloped dsDNA viruses (e.g. Herpesviruses: 1.15 g/mL). KV was estimated to be approximately 650-fold higher titre than DAV at 1.17 g/mL, and we were unable to identify intact DAV particles by electron microscopy (KV shown in Figure 1B). KV is morphologically similar to Oryctes rhinoceros nudivirus (Huger, 2005), with an enveloped rod-shaped virion approximately 200 nm long and 50 nm wide. Aliquots of the virus are available from the authors on request.

Kallithea Virus growth in flies

We injected the KV isolate into *Drosophila Oregon R* males and females, with and without *Wolbachia*, and measured viral titre at four timepoints by qPCR. In females, KV increased approximately 45,000-fold by day 10 (in females), and then began to decrease (Figure 1C). In males, the KV growth pattern was altered, growing more slowly (or possibly peaking at an earlier un-sampled time point), resulting in a 7-fold lower titre than in females after 10-15 days, (nominal MCMC p-value derived from posterior samples, MCMCp= 0.002). *Wolbachia* did not affect growth rate in either sex (MCMCp = 0.552, Figure S1), reaffirming previous findings

that *Wolbachia* do not offer the same protection against DNA viruses in *Drosophila* as they do against RNA viruses (Teixeira et al, 2008).

Nudiviruses have previously been reported to spread through sexual and faecal-oral transmission routes. The *Drosophila innubila* Nudivirus (DiNV), a close relative of KV, is thought to spread faecal-orally, so we tested whether KV can spread through infected food. We found that although oral transmission occurred, it was relatively inefficient (Figure 1D). However, the concentration of DiNV found in *D. innubila* faeces is broadly similar our KV isolate after gradient centrifugation (Unckless 2011; Figure 1D), and the administered suspension had been diluted 50-fold and may provide a lower dose than flies encounter naturally. To explore the potential for transovarial vertical transmission or gonad-specific infections following sexual transmission (as reported for Helicoverpa nudivirus 2; Burand et al, 2012), we also performed qPCR on dissected ovaries and the remaining carcasses at 3 DPI (Figure S2). We found that KV was highly enriched in the carcass relative to the ovaries. Although intra-abdominal injection could influence KV tissue-specificity, there were still substantial levels of KV in the ovaries, indicating there is not a complete barrier to infection. These results imply that KV is more likely to transmit faecal-orally than transovarially or through gonad-specific infections, but explicit tests for transovarial or sexual transmission are required.

Sex-specific mortality, lethargy, and altered fecundity patterns following KV infection

Drosophila innubila infected with DiNV suffer fitness costs including increased mortality and decreased fecundity (Unckless 2011). We investigated KV-induced mortality in *D. melanogaster* by injecting males and females, with and without *Wolbachia*, with either control gradient solution or KV. We found that KV caused slightly, but significantly, increased mortality in females compared with controls (21% dead by day 20, vs. 11% in controls, MCMCp = 0.001), but caused a dramatically increased mortality in males compared to females (63% dead by day 20, vs. 14% in controls, sex:virus interaction MCMCp < 0.0001; Figure 2A). Therefore, males appear less tolerant of infection by KV, displaying increased mortality and a lower titre than females. We confirmed the KV-induced male death was not caused by DAV or other unknown small unenveloped RNA viruses present in our initial isolate, as chloroform treatment of the KV isolate eliminated the effect (Figure S3). Male-specific costs of infection are widespread across animal hosts and their pathogens (e.g. Zuk, 2009), and reduced male tolerance has been found in flies infected with Drosophila C Virus (DCV) (Gupta and Vale, 2017). *Wolbachia* infection has previously been reported to affect resistance and tolerance to

RNA viruses but not a DNA virus (Teixeira et al, 2008). We found that *Wolbachia* had no detectable effect on KV-induced mortality in males or females, and thus does not affect tolerance (MCMCp = 0.20; Figure S1).

We next tested whether female flies suffer sub-lethal fitness costs by monitoring fly movement for a week following infection. KV-infected female flies showed similar movement patterns to chloroform-treated KV-injected flies for two days post-infection, but from three days post-infection moved significantly less (~70% reduction relative to controls; MCMCp < 0.001; Figure 2B). We conclude that females suffer from increased lethargy resulting from KV infection. In a natural setting, this could translate into fitness costs associated with increased predation, and reduced egg dispersal, mating, and foraging.

Finally, we tested whether KV infection resulted in decreased fecundity by monitoring the number of eggs laid for 12 days post-infection. We found that although there was no significant difference in the total number of eggs laid across the 12 days (MCMCp = 0.31), infected females exhibited markedly different egg laying patterns (MCMCp < 0.001; Figure 2). The first day following infection, infected flies laid 2.2-fold (95% HPD 1.4 to 3.3-fold) more eggs than uninfected flies, on average, while from days 4-12, KV-infected flies consistently laid fewer eggs than uninfected flies. However, when we repeated this experiment under similar conditions, we did not observe an increase in eggs laid on the first day post-infection, suggesting the result is inconsistent or that our first observation was a type I error. However, were able to confirm the reduction in eggs laid later in infection, supporting the conclusion that KV reduces late-life fecundity.

The reduction in egg-laying during late infection could be due to a behavioural response or a cessation of oogenesis. To differentiate between these possibilities, we dissected ovaries, and determined the proportion of ovarioles that contained mature egg chambers. We found that ovaries from KV-infected flies halt oogenesis around stage 8 (MCMCp < 0.001), before vitellogenesis, and house an increased number of apoptotic egg chambers (MCMCp < 0.001) (Figure 2). This phenotype is similar to that seen upon starvation (Jouandin et al, 2014), and could be the manifestation of a trade-off to reroute resources to fighting infection or sickness-induced anorexia (e.g. Ayres and Schneider, 2009). Alternatively, this could be a direct consequence of viral infection, consistent with the gonadal atrophy caused by HzNV-2 (Burand et al, 2012). Future studies should address whether this phenotype is a direct or indirect consequence of infection, and if the latter, whether it is orchestrated by the host or the virus.

Variation in titre and mortality following KV infection

The DGRP (Mackay et al, 2012) have previously been used to dissect genetic variation underlying resistance and tolerance to bacterial, fungal, and viral pathogens (Magwire et al, 2012; Maroun et al, 2015; Wang et al, 2017; Howick and Lazzaro, 2017). We infected 125 DGRP lines with KV and estimated broad-sense heritabilities (H^2: the proportion of phenotypic variance attributable to genetic line) and coefficients of genetic variation (CV_G: a mean-standardised measure of genetic variation) in viral titre, LT50 values in females, and LT50 values in males (Table 1). Our estimates of H^2 and CV_G fall within the range found for resistance to other pathogens in the DGRP, although direct comparison is difficult as studies are inconsistent in the statistics used to report genetic variation. H^2 in survival following infection with an opportunistic bacterium or fungus was similar to our estimate for survival following KV infection (*Pseudomonas aeruginosa*: H^2 in males = 0.47, H^2 in females = 0.38; *Metarhizium anisopliae*: H^2 in males = 0.23, H^2 in females = 0.27; Wang et al, 2017), although comparing heritability can be easily confounded by differences in environmental (residual) variance (Houle, 1992). Genetic variation in resistance has also been measured in response to two non-native *D. melanogaster* viruses (Flock House Virus and *Drosophila affinis* Sigma Virus) and two native viruses (DCV and DmelSV) in females of the DGRP. Of these, the lowest heritabilities are those associated with resistance to non-native fly viruses (FHV: $h^2 = 0.07$, $CV_G = 7$; *D. affinis* sigma virus: $h^2 = 0.13$), and the highest are associated with native fly viruses (DCV: $h^2 = 0.34$, $CV_G = 20$; DmelDV: $h^2 = 0.29$). Although Magwire et al (2012) inferred narrow sense heritability (h^2) as half V_G and accounted for the homozygosity of inbred lines when inferring CV_G, it is clear that V_G for resistance to KV is closer to the V_G for resistance to other native fly viruses than to non-native ones, at least for survival. It is also interesting to note that CV_G estimates for survival are higher than estimates for titre, consistent with the observation that traits more closely related to fitness are expected to have higher CV_G values (Houle, 1992).

We calculated genetic correlations between male and female mortality, and between viral titre and mortality in females (Figure 3). Note, we find no correlation between survival time following KV infection and published estimates of longevity in the absence of infection, nor to resistance to any other RNA viruses (Ivanov et al, 2015; Magwire et al, 2012). We find a strong positive correlation between males and females in median survival time following KV infection (0.57 [0.34-0.78]; MCMCp <0.001), such that that lines in which infected males die quickly are also lines in which infected females die quickly, suggesting a shared genetic basis for early

lethality following infection. We also surprisingly find a positive genetic correlation between viral titre and LT50 values (r = 0.32 [0.05-0.59], MCMCp = 0.017), such that fly lines that achieved higher titres on day 8 tend to live longer. However, the effect size is small (doubling of viral titre leads to a half-day increase in median survival time) and the result is only marginally significant. The absence of a negative correlation is counter-intuitive, and contrasts with infection of the DGRP with *Providencia rettgeri* and *Metarhizium anisopliae*, and infection across *Drosophila* species with DCV, where fly lines or species with higher loads suffer increased mortality (Longdon et al, 2015; Wang et al, 2017; Howick and Lazzaro, 2017). The apparent decoupling of titre and mortality could result from inherent costs associated with the immune response, whereby flies that raise a more potent immune response keep KV at lower titres but induce greater tissue damage.

Identification of candidate genes underlying host variation in KV titre

Using the phenotypes in the DGRP lines measured above, we performed a genome-wide association study to identify candidate genes underlying variation in titre, LT50, and differences in LT50 between the sexes. We found 10 SNPs (9 near genes) which were significantly (p_{sim} < 0.05, based on 1000 permutations of phenotypes across lines) associated with viral titre (Figure 4). The SNP with the smallest p-value appeared in *Lipophorin receptor 2* (*LpR2*), which encodes a low-density lipoprotein receptor, previously found to be broadly required for flavivirus and rhabdovirus cell entry (e.g. Agnello et al, 1999; Albecka et al, 2012; Finkelshtein et al, 2013).

We tested whether these candidate polymorphisms were enriched in any molecular, biological, or cellular processes using a GO enrichment analysis, and found the top hit to be the torso signalling pathway with 2 genes of 34 in the category (p = 0.0004), *tailless* and *daughter of sevenless* (*dos*). Torso signalling is upstream of extracellular-signal-regulated kinase (ERK) pathway activation in some tissues, and human orthologues of *dos* (GAB1/GAB2/GAB4) are cleaved by an enterovirus-encoded protease, thereby activating ERK signalling and promoting viral replication (Deng et al 2015; Deng et al, 2017). ERK signalling is also an important regulator of virus replication in the fly and mosquito midguts, where it couples nutrient availability with antiviral activity (Xu et al, 2013; Liu et al, 2017). See Table S1 for a list of all nominally significant SNPs with associated locations, mutation types (e.g. intronic, synonymous coding, etc), nearby genes, p-values, effect sizes, and GO terms.

Identification of candidate genes underlying host variation in KV-induced mortality

We found 86 SNPs (65 near genes) that were significantly ($p_{sim} < 0.05$) associated with LT50 following KV infection in the DGRP (Figure 4, Table S1), none of which were identified in the GWAS for viral titre. We performed a GO enrichment analysis, and found genes associated with these SNPs were enriched for hydrolase activity (top molecular function GO term, p = 0.0004), stem cell fate determination (top biological process GO term, p = 0.002), and in the plasma membrane (top cell component GO term, p = 0.004), among others (Table S2). Of these 86 SNPs, we found 34 (26 near genes) that were highly significant ($p_{sim} < 0.01$), and selected these for further analysis and confirmation (see all significant SNPs in Table S1). The polymorphism with the most confident association was located in *Cdc42-interacting protein 4* (*Cip4*), a gene involved in membrane remodelling and endocytosis (Leibfried et al, 2008; Fricke et al, 2009). This SNP is intronic in the majority of *Cip4* transcripts, but represents a nonsynonymous polymorphism segregating leucine and proline in the first exon of *Cip4-PB* and *Cip4-PD* isoforms, perhaps indicating spliceoform-specific effects on KV-induced mortality. Of particular interest from the remaining 33 highly significant SNPs was a synonymous SNP in the receptor tyrosine kinase, *sevenless*, known to interact with *dos* (above), and seven genes (*Dgk, Atg10, ATPCL, Hppy, Pkcdelta, Gprk2, Pdcd4*) previously implicated in viral pathogenesis or general immune processes. Of these, three (*Gprk4, hppy, Pkcdelta*) are involved in NFκB signalling (Valanne et al, 2011, Chuang et al, 2011; Loegering and Lennartz, 2011). *ATPCL* was identified in an RNAi screen for factors regulating Chikungunya virus replication in humans (Karlas et al, 2016) and is involved in the late replication complexes of Semliki Forest Virus (Varjak et al, 2013). Finally, *Atg10* and *Pdcd4* are involved in autophagy and apoptosis, respectively, both broadly antiviral cellular functions known to have a role in antiviral immunity in *Drosophila* (Shelly et al, 2009; Lamiable and Imler, 2014). We found no SNPs significantly associated with sex-specific KV-induced mortality (Figure S4).

Confirmation of GWAS hits

We chose 19 GWAS-candidate genes with available UAS-driven RNAi constructs to verify their involvement in KV infection. The only gene independently confirmed by both GAL4 drivers (i.e. *tub-GAL4* and *myo31DF-GAL4*) was *Cip4*, the top hit in the mortality GWAS (Figure 5). We observed an increase in viral titre when *Cip4* was knocked down in the entire fly (*tub-GAL4*, 5-fold increase, 95% C.I. 1-30 fold, MCMCp = 0.02), or specifically in the gut (*myo31DF-GAL4*, 63-fold increase, 95% C.I. 3-1290 fold, MCMCp = 0.006, Figure 5). It is known that baculovirus budded virions enter cells through clathrin-mediated endocytosis or micropinocytosis (Long et al, 2006; Kataoka et al, 2012), and gain their envelope at the cell membrane upon exit (Blissard and Rohrmann, 1990). Thus, Cip4 could plausibly enact an

antiviral effect by limiting KV cell entry or spread, perhaps through its known function in cell membrane remodelling and trafficking. In addition to *Cip4*, whole-fly knockdown of *CG12821* caused a marginally significant increase in viral titre (7.4-fold increase, MCMCp = 0.034, Figure 5), although the cross with *myo31DF-GAL4* proved lethal. Finally, five genes (*btd*, *PKCdelta*, *Gprk2*, *LpR2*, and *tll*) exhibited significantly increased, albeit highly variable, viral titre when knocked down using the *myo31DF-GAL4* driver, but not the *tub-GAL4* driver, perhaps indicating differences in GAL4 efficiency and a gut-specific requirement for these genes. Notably, these five genes include two Toll-associated factors, and *LpR2*, the top hit from the titre GWAS.

Immune genes differentially expressed following KV infection

Previous transcriptional profiling in response to DCV infection has shown upregulation of heatshock proteins, JAK-STAT, JNK, and Imd pathways (Zhu et al, 2013; Merkling et al, 2015). However, the *D. melanogaster* expression response to a DNA virus has not previously been investigated. We separately injected male and female flies with control gradient solution or KV, and extracted mRNA for sequencing 3 days post-infection. Three days-post infection, KV gene expression increased drastically, consistent with our qPCR analysis of genome copy-number (Figure 1, Figure S8). Using a Benjamini–Hochberg adjusted significance threshold of $p < 0.05$, and a fold change threshold of 2, we found 120 genes upregulated and 458 genes downregulated in response to KV in either males or females (Figure 6; Table S3). Principal components analysis on depth-normalised read counts separated males and females along PC1 and partially separated KV-infected and control-injected libraries along PC3 (Figure S5).

We observed differential expression of immune genes in JAK-STAT, Toll, IMD, and RNAi pathways relative to gradient controls in both sexes (Figure 7, Figure S7). Of note, JAK-STAT ligands *upd2* and *upd3* were significantly upregulated. Toll components were generally upregulated, including ligands *spz* and *spz3*, NFκB homologue *dorsal*, and upstream pattern recognition receptor *PGRP-SA*. The IMD pathway appeared activated in response to KV, as evidenced by upregulation of the two DIAP genes (*Diap1* – downstream of IMD, *Diap2* – upstream of IMD), upregulation of two IKK genes (*IKKbeta* and *kenny*), and downregulation of the inhibitory cytokine *Diedel3* and inhibitory *PGRP-SC* receptors. Although the IMD and Toll pathways seemed active, 13 of the 14 differentially expressed antimicrobial peptides were downregulated, perhaps due to pathogen-specificity in immune pathways or virus encoded suppressors of NFκB signalling (Lamiable et al, 2015). We found RNAi effector *AGO2* was upregulated, consistent with the previous results that DNA viruses are a target of the RNAi pathway (Kemp et al, 2012; Bronkhorst et al, 2012; Bronkhorst et al, 2014). Strikingly, *Vago*,

an antiviral factor induced by Dicer-2 (Deddouche et al, 2008), was upregulated and was also adjacent to a SNP found in the mortality GWAS (*dos*; Figure 4, Figure 7). We also found that *pastrel* and *ref(2)P* were differentially expressed, both genes identified in previous genome wide association analyses for resistance to DCV and DMelSV, respectively. Finally, we found that KV induced expression of *CG1667*, the *Drosophila* homologue of STING. The vertebrate cGAS-STING pathway is involved in cytosolic DNA sensing and activation of immune factors in response to DNA virus infection (Chen et al, 2016), and the upregulation of *CG1667* may suggest that this is another pathway conserved between *Drosophila* and vertebrates.

Other genes differentially expressed following KV infection

In addition to the differentially expressed immune genes described above, we also identified an enrichment of differentially expressed genes involved in serine endo-peptidase activity (top molecular function GO term, $p = 6.4x10^{-13}$) and chitin-based cuticle development (top biological process GO term, $p = 6.9x10^{-5}$). Although not necessarily immune related, these have previously been identified in expression analyses in response to DMelSV in flies and baculovirus infection of moths (Carpenter, Hutter et al, 2009; McTaggart et al, 2015). In baculoviruses, the chitin-binding vp91 is specifically required for midgut infection, and is believed to bind the peritrophic matrix to mediate cell entry (Rohrmann, 2013; Lemaitre and Miguel-Aliaga, 2013). As KV encodes a *vp91* homologue and is able to orally infect flies (Figure 1), it seems likely that upregulation of chitin-based cuticle proteins occurs in the gut following infection. Upregulation of cuticle proteins was in part due to the striking upregulation of 11 of the 24 Tweedle genes (Figure S6) in some (but not all) of the infected samples. These are secreted, insect-specific cuticle proteins involved in body shape (Guan et al, 2006), and are also upregulated in response to Sindbis virus infection in cell culture (Graveley et al, 2011, Pers Comm to Flybase), perhaps suggesting a general role in viral pathogenesis.

Genes with altered differential expression between males and females

As we had observed male and female differences in KV-induced mortality and titre (Figure 1, Figure 2), we tested for sex-specific transcriptional regulation in response to KV infection. We found 64 genes are differentially expressed between the sexes specifically in response to KV (Table S3). Most genes with sex-specific regulation are those downregulated in females, and these were highly enriched for genes associated with the chorion (top cellular component GO term, $p = 5.45x10^{-26}$; Figure 6, Table S4). Strikingly, all but three genes classified with the GO term ‘chorion’ were downregulated in females (Figure 5), and females downregulated 300 genes that were not significantly downregulated in males. This implies a

substantial reorganization of oogenesis and is consistent with the observed reduction in eggs laid after day three (Figure 2). We did not identify any previously described immune genes with sex-specific regulation during KV infection.

Although the interaction term between sex and KV treatment was not significant for many genes (Figure 6A), we noticed that very few genes were upregulated in response to KV in males. Upon closer inspection, we found many of these genes represent general differences between uninfected male and female transcriptomes (Figure 6). For example, of the 96 KV responsive genes upregulated in females but not males, we found that 75 have male-biased expression in uninfected flies, with 54 of those having significantly greater expression in males, both of which are greater than would be expected by chance (bootstrap $p < 0.001$, for both) (Figure 6). This result holds when excluding genes that are ovary or testis-specific, indicating this is not driven by the dramatic downregulation of oogenesis-related genes. These data suggest males may have a baseline expression profile that is more prepared for infection, and could explain the lower titre differences we observe in males relative to females.

Conclusions

We have isolated Kallithea Virus, a dsDNA nudivirus that naturally infects *D. melanogaster*, and find it experimentally tractable. KV infection leads to reduced fertility and movement in females, highlighting the importance of measuring fitness associated traits besides longevity. Although males suffered greater mortality than females, they sustained lower titres, and had higher basal expression of KV-responsive genes, consistent with increased resistance and/or reduced tolerance in males. Similar to RNA viruses, we identified moderate host genetic variation in resistance to KV infection, however, we found that the underlying genetic architecture of this variation is unlike previously studied RNA viruses of *D. melanogaster*, in which a high proportion of genetic variation was determined by a small number of loci. This could reflect a difference in the co-evolutionary dynamics between *D. melanogaster* and KV, versus other RNA viruses such as DCV and DMelSV. KV infection also induced expression changes in the JAK-STAT, IMD, Toll, and RNAi pathways, which are known to have antiviral roles against RNA viruses, indicating DNA antiviral immunity relies on previously studied invertebrate immune pathways. However, widespread downregulation of AMPs, upregulation of cuticle proteins, and downregulation of chorion factors could represent infection responses distinctive to DNA viruses or KV. Notably, upregulation of the *Drosophila* STING orthologue is consistent with this pathway having a conserved function in DNA virus sensing from flies to

mammals, confirming the continued utility of the *Drosophila* system for understanding host-virus interaction and coevolution.

Acknowledgements

We thank John Pool for the original fly collection that contained the KV isolate; Megan Wallace, Steve Mitchell, and Naomi Letley for help with experimental work; Pedro Vale, Katy Monteith, and Fergal Waldron for creation, upkeep, and sharing of the outbred DGRP population; Craig Walling and Jarrod Hadfield for statistical advice, and members of the Obbard and Vale labs for discussion.

Funding

WHP is supported by the Darwin Trust of Edinburgh, this work was partly supported by a Wellcome Trust Research Career Development fellowship to DJO (WT085064) and a Wellcome Trust strategic award to the Centre for Immunity, Infection and Evolution (WT095831). Use of the transmission electron microscope was supported by a Wellcome Trust Multi User Equipment Grant (WT104915MA). PB was supported by the BBSRC-funded Institute Strategic Programme Pathogenesis & Resistance in Viral Diseases of Livestock [BB/J004324/1].

References

Agnello, V., G. Abel, M. Elfahal, G. B. Knight, and Q. X. Zhang, 1999 Hepatitis C virus and other flaviviridae viruses enter cells via low density lipoprotein receptor. Proc. Natl. Acad. Sci. U. S. A. 96: 12766–71.

Albecka, A., S. Belouzard, A. O. de Beeck, V. Descamps, L. Goueslain *et al.*, 2012 Role of low-density lipoprotein receptor in the hepatitis C virus life cycle. Hepatology 55: 998–1007.

Anders, S., and W. Huber Differential expression analysis for sequence count data.

Avadhanula, V., B. P. Weasner, G. G. Hardy, J. P. Kumar, and R. W. Hardy, 2009 A Novel System for the Launch of Alphavirus RNA Synthesis Reveals a Role for the Imd Pathway in Arthropod Antiviral Response (S.-W. Ding, Ed.). PLoS Pathog. 5: e1000582.

Ayres, J. S., and D. S. Schneider, 2009 The Role of Anorexia in Resistance and Tolerance to Infections in Drosophila (D. Promislow, Ed.). PLoS Biol. 7: e1000150.

Blissard, G. W., and G. F. Rohrmann, 1990 Baculovirus Diversity and Molecular Biology. Annu. Rev. Entomol. 35: 127–155.

Breitenbach, J. E., K. S. Shelby, and H. J. R. Popham, 2011 Baculovirus Induced Transcripts in Hemocytes from the Larvae of Heliothis virescens. Viruses 3: 2047–2064.

Bronkhorst, A. W., K. W. R. van Cleef, H. Venselaar, and R. P. van Rij, 2014 A dsRNA-binding protein of a complex invertebrate DNA virus suppresses the Drosophila RNAi response. Nucleic Acids Res. 42: 12237–12248.

Bronkhorst, A. W., K. W. R. van Cleef, N. Vodovar, I. A. Ince, H. Blanc *et al.*, 2012 The DNA virus Invertebrate iridescent virus 6 is a target of the Drosophila RNAi machinery. Proc. Natl. Acad. Sci. 109: E3604–E3613.

Brun, P., and N. Plus, 1980 The viruses of Drosophila, pp. 625–702 in *The genetics and biology of Drosophila*,.

Burand, J. P., W. Kim, C. L. Afonso, E. R. Tulman, G. F. Kutish *et al.*, 2012 Analysis of the Genome of the Sexually Transmitted Insect Virus Helicoverpa zea Nudivirus 2. Viruses 4: 28–61.

Carpenter, J., S. Hutter, J. F. Baines, J. Roller, S. S. Saminadin-Peter *et al.*, 2009 The transcriptional response of Drosophila melanogaster to infection with the sigma virus (Rhabdoviridae). PLoS One 4: e6838.

Chen, Q., L. Sun, and Z. J. Chen, 2016 Regulation and function of the cGAS–STING pathway of cytosolic DNA sensing. Nat. Immunol. 17: 1142–1149.

Chuang, H.-C., J.-L. Lan, D.-Y. Chen, C.-Y. Yang, Y.-M. Chen *et al.*, 2011 The kinase GLK controls autoimmunity and NF-?B signaling by activating the kinase PKC-? in T cells. Nat. Immunol. 12: 1113–1118.

Clemmons, A. W., S. A. Lindsay, and S. A. Wasserman, 2015 An effector Peptide family required for Drosophila toll-mediated immunity. (N. Silverman, Ed.). PLoS Pathog. 11: e1004876.

Cogni, R., C. Cao, J. P. Day, C. Bridson, and F. M. Jiggins, 2016 The genetic architecture of resistance to virus infection in *Drosophila*. Mol. Ecol. 25: 5228–5241.

Compton, A. A., V. M. Hirsch, and M. Emerman, 2012 The host restriction factor APOBEC3G and retroviral Vif protein coevolve due to ongoing genetic conflict. Cell Host Microbe 11: 91–8.

Contamine, D., A. M. Petitjean, and M. Ashburner, 1989 Genetic resistance to viral infection: the molecular cloning of a Drosophila gene that restricts infection by the rhabdovirus sigma. Genetics 123: 525–33.

Deddouche, S., N. Matt, A. Budd, S. Mueller, C. Kemp *et al.*, 2008 The DExD/H-box helicase Dicer-2 mediates the induction of antiviral activity in drosophila. Nat. Immunol. 9: 1425–1432.

Deng, H., G. Fung, Y. Qiu, C. Wang, J. Zhang *et al.*, 2017 Cleavage of Grb2-Associated Binding Protein 2 by Viral Proteinase 2A during Coxsackievirus Infection. Front. Cell. Infect. Microbiol. 7: 85.

Deng, H., G. Fung, J. Shi, S. Xu, C. Wang *et al.*, 2015 Enhanced enteroviral infectivity via viral protease-mediated cleavage of Grb2-associated binder 1. FASEB J. 29: 4523–31.

Dobin, A., C. A. Davis, F. Schlesinger, J. Drenkow, C. Zaleski *et al.*, 2013 STAR: ultrafast universal RNA-seq aligner. Bioinformatics 29: 15–21.

Dostert, C., E. Jouanguy, P. Irving, L. Troxler, D. Galiana-Arnoux *et al.*, 2005 The Jak-STAT signaling pathway is required but not sufficient for the antiviral response of drosophila. Nat. Immunol. 6: 946–953.

Dupuis, S., E. Jouanguy, S. Al-Hajjar, C. Fieschi, I. Z. Al-Mohsen *et al.*, 2003 Impaired response to interferon-α/β and lethal viral disease in human STAT1 deficiency. Nat. Genet. 33: 388–391.

Feng, Z., L. Hensley, K. L. McKnight, F. Hu, V. Madden *et al.*, 2013 A pathogenic picornavirus acquires an envelope by hijacking cellular membranes. Nature 496: 367–71.

Ferguson, H. M., and A. F. Read, 2002 Why is the effect of malaria parasites on mosquito survival still unresolved? Trends Parasitol. 18: 256–261.

Finkelshtein, D., A. Werman, D. Novick, S. Barak, and M. Rubinstein, 2013 LDL receptor and its family members serve as the cellular receptors for vesicular stomatitis virus. Proc. Natl. Acad. Sci. U. S. A. 110: 7306–11.

Fricke, R., C. Gohl, E. Dharmalingam, A. Grevelhörster, B. Zahedi *et al.*, 2009 Drosophila Cip4/Toca-1 Integrates Membrane Trafficking and Actin Dynamics through WASP and SCAR/WAVE. Curr. Biol. 19: 1429–1437.

Gauthier, J., J.-M. Drezen, and E. A. Herniou, 2017 The recurrent domestication of viruses: major evolutionary transitions in parasitic wasps. Parasitology 1–13.

Graveley, B. R., A. N. Brooks, J. W. Carlson, M. O. Duff, J. M. Landolin *et al.*, 2011 The developmental transcriptome of Drosophila melanogaster. Nature 471: 473–479.

Guan, X., B. W. Middlebrooks, S. Alexander, and S. A. Wasserman, 2006 Mutation of TweedleD, a member of an unconventional cuticle protein family, alters body shape in Drosophila. Proc. Natl. Acad. Sci. U. S. A. 103: 16794–9.

Gupta, V., C. O. Stewart, S. S. C. Rund, K. Monteith, and P. F. Vale, 2017 Costs and benefits of sublethal Drosophila C virus infection. J. Evol. Biol. 30: 1325–1335.

Gupta, V., and P. F. Vale, 2017 Nonlinear disease tolerance curves reveal distinct components of host responses to viral infection. R. Soc. open Sci. 4: 170342.

Hadfield, J. D., 2010 MCMC Methods for Multi-Response Generalized Linear Mixed Models: The MCMCglmm R Package. J. Stat. Softw. 33: 1–22.

Herniou, E. A., E. Huguet, J. Thézé, A. Bézier, G. Periquet *et al.*, 2013 When parasitic wasps hijacked viruses: genomic and functional evolution of polydnaviruses. Philos. Trans. R. Soc. Lond. B. Biol. Sci. 368: 20130051.

Herniou, E. A., J. A. Olszewski, D. R. O'Reilly, and J. S. Cory, 2004 Ancient coevolution of baculoviruses and their insect hosts. J. Virol. 78: 3244–51.

Hill, T., and R. Unckless, 2017 The dynamic evolution of Drosophila innubila Nudivirus. doi.org 197293.

Houle, D., 1992 Comparing evolvability and variability of quantitative traits. Genetics 130: 195–204.

Howick, V. M., and B. P. Lazzaro, 2017 The genetic architecture of defence as resistance to and tolerance of bacterial infection in Drosophila melanogaster. Mol. Ecol. 26: 1533–1546.

Huger, A. M., 2005 The Oryctes virus: its detection, identification, and implementation in biological control of the coconut palm rhinoceros beetle, Oryctes rhinoceros (Coleoptera: Scarabaeidae). J. Invertebr. Pathol. 89: 78–84.

Huszar, T., and J. Imler, 2008 Chapter 6 Drosophila Viruses and the Study of Antiviral Host-Defense, pp. 227–265 in *Advances in virus research*,.

Ivanov, D. K., V. Escott-Price, M. Ziehm, M. M. Magwire, T. F. C. Mackay *et al.*, 2015 Longevity GWAS Using the *Drosophila* Genetic Reference Panel. Journals Gerontol. Ser. A Biol. Sci. Med. Sci. 70: 1470–1478.

Jouandin, P., C. Ghiglione, and S. Noselli, 2014 Starvation induces FoxO-dependent mitotic-to-endocycle switch pausing during Drosophila oogenesis. Development 141: 3013–3021.

Kataoka, C., Y. Kaname, S. Taguwa, T. Abe, T. Fukuhara *et al.*, 2012 Baculovirus GP64-mediated entry into mammalian cells. J. Virol. 86: 2610–20.

Kemp, C., S. Mueller, A. Goto, V. Barbier, S. Paro *et al.*, 2013 Broad RNA interference-mediated antiviral immunity and virus-specific inducible responses in Drosophila. J. Immunol. 190: 650–8.

King, E. G., and A. D. Long, 2017 The Beavis Effect in Next-Generation Mapping Panels in Drosophila melanogaster. G3 Genes, Genomes, Genet. 7.:

Lamiable, O., and J.-L. Imler, 2014 Induced antiviral innate immunity in Drosophila. Curr. Opin. Microbiol. 20: 62–68.

Lamiable, O., C. Kellenberger, C. Kemp, L. Troxler, N. Pelte *et al.*, 2016 Cytokine Diedel and a viral homologue suppress the IMD pathway in Drosophila. Proc. Natl. Acad. Sci. U. S. A. 113: 698–703.

Lee, Y. S., K. Nakahara, J. W. Pham, K. Kim, Z. He *et al.*, 2004 Distinct Roles for Drosophila Dicer-1 and Dicer-2 in the siRNA/miRNA Silencing Pathways. Cell 117: 69–81.

Leibfried, A., R. Fricke, M. J. Morgan, S. Bogdan, and Y. Bellaiche, 2008 Drosophila Cip4 and WASp define a branch of the Cdc42-Par6-aPKC pathway regulating E-cadherin endocytosis. Curr. Biol. 18: 1639–48.

Lemaitre, B., and I. Miguel-Aliaga, 2013 The Digestive Tract of *Drosophila melanogaster*. Annu. Rev. Genet. 47: 377–404.

Li, Y., J. Lu, Y. Han, X. Fan, and S.-W. Ding, 2013 RNA Interference Functions as an Antiviral Immunity Mechanism in Mammals. Science (80-.). 342.:

Liao, Y., G. K. Smyth, and W. Shi, 2013 The Subread aligner: fast, accurate and scalable read mapping by seed-and-vote. Nucleic Acids Res. 41: e108–e108.

Liu, X., J. J. Hodgson, and N. Buchon, 2017 Drosophila as a model for homeostatic, antibacterial, and antiviral mechanisms in the gut (K. A. Kline, Ed.). PLOS Pathog. 13: e1006277.

Loegering, D. J., and M. R. Lennartz, 2011 Protein kinase C and toll-like receptor signaling. Enzyme Res. 2011: 537821.

Long, G., X. Pan, R. Kormelink, and J. M. Vlak, 2006 Functional entry of baculovirus into insect and mammalian cells is dependent on clathrin-mediated endocytosis. J. Virol. 80: 8830–3.

Longdon, B., J. D. Hadfield, J. P. Day, S. C. L. Smith, J. E. McGonigle *et al.*, 2015 The causes and consequences of changes in virulence following pathogen host shifts. PLoS Pathog. 11: e1004728.

Longdon, B., J. D. Hadfield, C. L. Webster, D. J. Obbard, and F. M. Jiggins, 2011 Host Phylogeny Determines Viral Persistence and Replication in Novel Hosts (D. S. Schneider, Ed.). PLoS Pathog. 7: e1002260.

Love, M. I., W. Huber, and S. Anders, 2014 Moderated estimation of fold change and dispersion for RNA-seq data with DESeq2. Genome Biol. 15.:

Mackay, T. F. C., S. Richards, E. A. Stone, A. Barbadilla, J. F. Ayroles *et al.*, 2012 The Drosophila melanogaster Genetic Reference Panel. Nature 482: 173–178.

Magwire, M. M., F. Bayer, C. L. Webster, C. Cao, and F. M. Jiggins, 2011 Successive Increases in the Resistance of Drosophila to Viral Infection through a Transposon Insertion Followed by a Duplication (D. J. Begun, Ed.). PLoS Genet. 7: e1002337.

Magwire, M. M., D. K. Fabian, H. Schweyen, C. Cao, B. Longdon *et al.*, 2012 Genome-Wide Association Studies Reveal a Simple Genetic Basis of Resistance to Naturally Coevolving Viruses in Drosophila melanogaster (M. L. Wayne, Ed.). PLoS Genet. 8: e1003057.

Maillard, P. V., C. Ciaudo, A. Marchais, Y. Li, F. Jay *et al.*, 2013 Antiviral RNA Interference in Mammalian Cells. Science (80-.). 342.:

Martin, M., 2011 Cutadapt removes adapter sequences from high-throughput sequencing reads. EMBnet.journal 17: 10.

Mctaggart, S. J., T. Hannah, S. Bridgett, J. S. Garbutt, G. Kaur *et al.*, 2011 Novel insights into the insect trancriptome response to a natural DNA virus.

Medd, N. C., S. Fellous, F. Waldron, M. Nakai, A. Xuereb *et al.*, 2017 The virome of Drosophila suzukii, an invasive pest of soft fruit. doi.org 190322.

Merkling, S. H., A. W. Bronkhorst, J. M. Kramer, G. J. Overheul, A. Schenck *et al.*, 2015 The epigenetic regulator G9a mediates tolerance to RNA virus infection in Drosophila. (P. F. Vale, Ed.). PLoS Pathog. 11: e1004692.

van Mierlo, J. T., G. J. Overheul, B. Obadia, K. W. R. van Cleef, C. L. Webster *et al.*, 2014 Novel Drosophila Viruses Encode Host-Specific Suppressors of RNAi (D. S. Schneider, Ed.). PLoS Pathog. 10: e1004256.

Nguyen, Q., L. K. Nielsen, and S. Reid, 2013 Genome scale transcriptomics of baculovirus-insect interactions. Viruses 5: 2721–47.

Noland, J., J. Breitenbach, H. Popham, S. Hum-Musser, H. Vogel *et al.*, 2013 Gut Transcription in Helicoverpa zea is Dynamically Altered in Response to Baculovirus Infection. Insects 4: 506–520.

Pfeiffenberger, C., B. C. Lear, K. P. Keegan, and R. Allada, 2010 Locomotor activity level monitoring using the Drosophila Activity Monitoring (DAM) System. Cold Spring Harb. Protoc. 2010: pdb.prot5518.

Rohrmann, G. F., 2013 The baculovirus replication cycle: Effects on cells and insects.

Sharma, S., B. R. tenOever, N. Grandvaux, G.-P. Zhou, R. Lin *et al.*, 2003 Triggering the Interferon Antiviral Response Through an IKK-Related Pathway. Science (80-.). 300.:

Shelly, S., N. Lukinova, S. Bambina, A. Berman, and S. Cherry, 2009 Autophagy is an essential component of Drosophila immunity against vesicular stomatitis virus. Immunity 30: 588–98.

Teixeira, L., A. Ferreira, and M. Ashburner, 2008 The bacterial symbiont Wolbachia induces resistance to RNA viral infections in Drosophila melanogaster. (L. Keller, Ed.). PLoS Biol. 6: e2.

Thézé, J., A. Bézier, G. Periquet, J.-M. Drezen, and E. A. Herniou, 2011 Paleozoic origin of insect large dsDNA viruses. Proc. Natl. Acad. Sci. U. S. A. 108: 15931–5.

Unckless, R. L., 2011 A DNA Virus of Drosophila (R. DeSalle, Ed.). PLoS One 6: e26564.

Valanne, S., J.-H. Wang, and M. Ramet, 2011 The Drosophila Toll Signaling Pathway. J. Immunol. 186: 649–656.

Varjak, M., S. Saul, L. Arike, A. Lulla, L. Peil *et al.*, 2013 Magnetic fractionation and proteomic dissection of cellular organelles occupied by the late replication complexes of Semliki Forest virus. J. Virol. 87: 10295–312.

Wang, X.-H., R. Aliyari, W.-X. Li, H.-W. Li, K. Kim *et al.*, 2006 RNA Interference Directs Innate Immunity Against Viruses in Adult Drosophila. Science (80-.). 312.:

Wang, Y., and J. A. Jehle, 2009 Nudiviruses and other large, double-stranded circular DNA viruses of invertebrates: New insights on an old topic. J. Invertebr. Pathol. 101: 187–193.

Webster, C. L., B. Longdon, S. H. Lewis, and D. J. Obbard, 2016 Twenty-Five New Viruses Associated with the Drosophilidae (Diptera). Evol. Bioinform. Online 12: 13–25.

Webster, C. L., F. M. Waldron, S. Robertson, D. Crowson, G. Ferrari *et al.*, 2015 The Discovery, Distribution, and Evolution of Viruses Associated with Drosophila melanogaster. PLoS Biol. 13: e1002210.

Williams, T., 2008 Natural invertebrate hosts of iridoviruses (Iridoviridae). Neotrop. Entomol. 37: 615–632.

Xu, J., and S. Cherry, 2014 Viruses and antiviral immunity in Drosophila. Dev. Comp. Immunol. 42: 67–84.

Xu, J., K. Hopkins, L. Sabin, A. Yasunaga, H. Subramanian *et al.*, 2013 ERK signaling couples nutrient status to antiviral defense in the insect gut. Proc. Natl. Acad. Sci. 110: 15025–15030.

Young, M. D., M. J. Wakefield, G. K. Smyth, and A. Oshlack, 2010 Gene ontology analysis for RNA-seq: accounting for selection bias. Genome Biol. 11: R14.

Zambon, R. A., M. Nandakumar, V. N. Vakharia, and L. P. Wu, 2005 The Toll pathway is important for an antiviral response in Drosophila. Proc. Natl. Acad. Sci. U. S. A. 102: 7257–62.

Zuk, M., 2009 The sicker sex. PLoS Pathog. 5: e1000267.

Figures

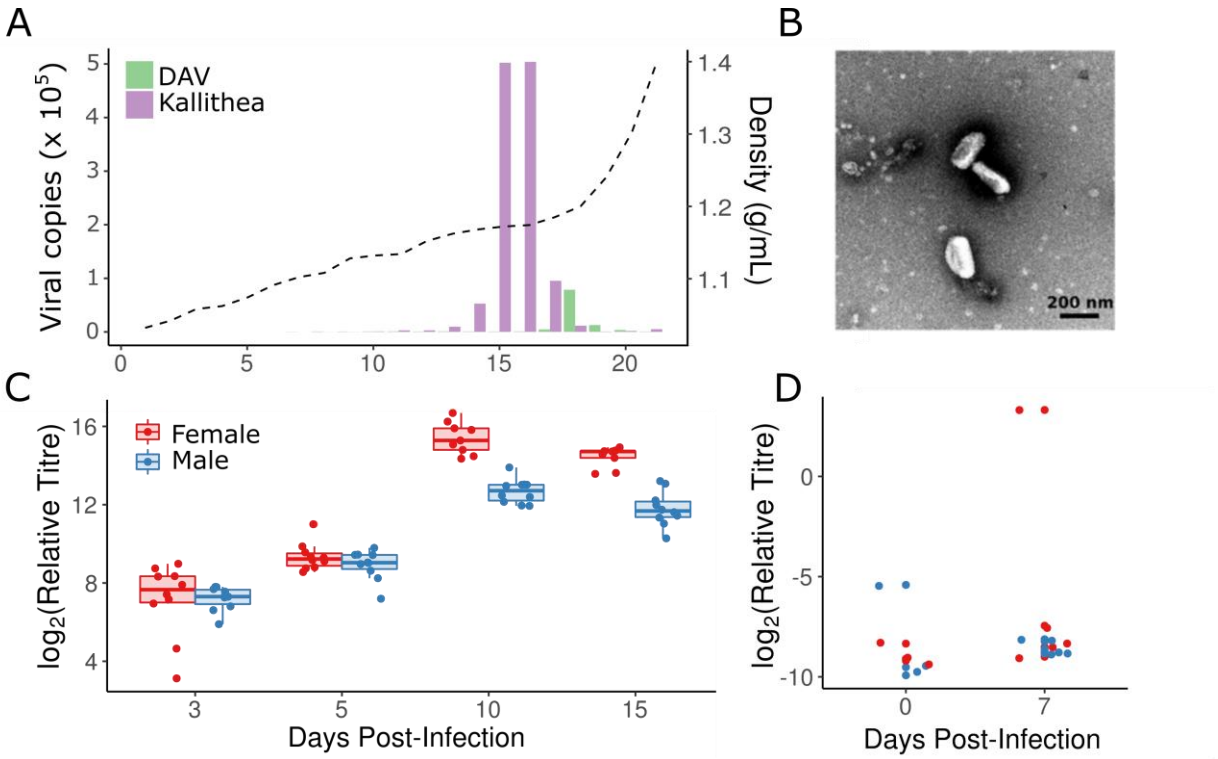

Figure 1: Isolation of KV and growth in flies

(A) Density gradient and virus titre: Kallithea virus (purple) was effectively separated from DAV (green) at 1.18 g/mL (dotted line) in fractions 15 and 16 of an iodixanol gradient. (B) Transmission electron micrograph of KV-positive fractions showed KV to be a rod-shaped enveloped particle, as has been described previously for other nudiviruses (Huger, 2005). We did not observe unenveloped particles, bacteria, or RNA viruses in the isolate. (C) Relative viral titres normalised by the number of fly genomic copies and virus levels at time zero in each sex. Each point represents a vial of 10 flies. Viral titres peaked at 10 days post-infection, and were generally higher in females (red) than males (blue) late in infection. (D) We were able to infect adult flies orally by applying the viral isolate to *Drosophila* medium, although relative copy number of the virus was very low and infection was inefficient, with only 2 of 16 vials (each of 10 flies) having increased titre after one week, indicating an infectious rate lower bound of ~1% at $5x10^3$ ID50.

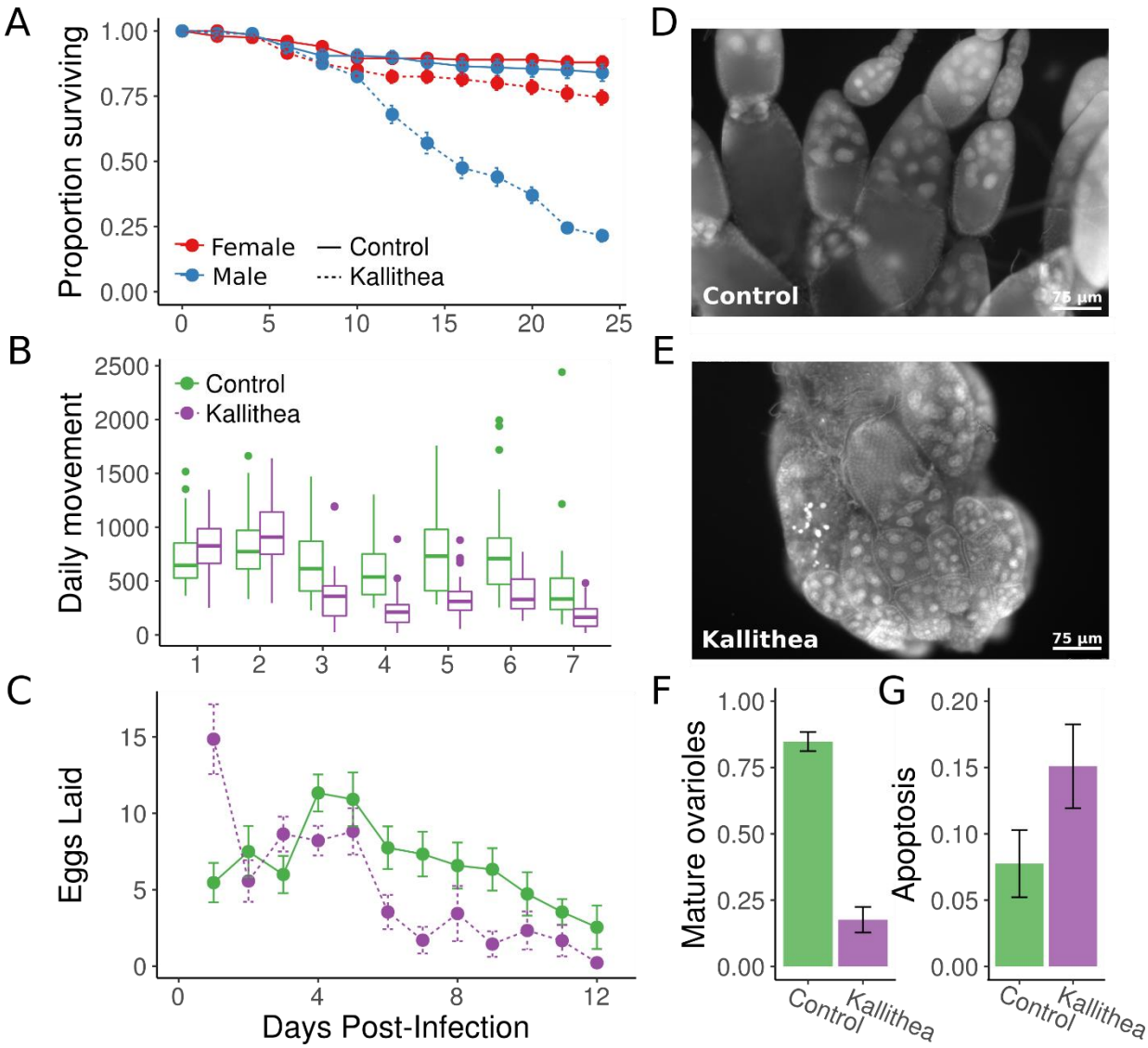

Figure 2: KV causes male-specific mortality, increased lethargy, and decreased fecundity
(A) Injection of KV virus into *OreR* flies led to sex-specific mortality. Infected females (red dotted line) experienced a small but significant increase in mortality, but males (blue dotted line) experienced a significantly larger rate of mortality after day 10. Flies injected with control gradient solution were unaffected (solid lines). Each point is the mean and standard error for the proportion of flies alive in each vial (10 vials of 10 flies). (B) Although females remained alive, they were more lethargic. We assessed daily movement of flies injected with either chloroform-inactivated KV (green) or active KV (purple). KV-infected flies moved less from days 3-7 post-infection. (C) Females also displayed altered egg laying behaviour. Fifteen pairs of flies were injected with inactive chloroform treated KV (green) or active KV (purple). KV-infected flies appeared to lay more eggs at the beginning of infection (although this was not replicated in a subsequent independent experiment), but did lay fewer eggs as infection progressed. This reduction in egg laying is due to a shutdown of oogenesis before vitellogenesis (D, E), and ovaries from KV-infected flies house a lower proportion of ovarioles that include late-stage and mature egg chambers (F) and a higher proportion which contain apoptotic nurse cells (G).

Trait	Mean	V_G	V_P	H^2	CV_G
Titre	1.96 [1.31 - 2.63]	0.05 [0.03 - 0.09]	0.28 [0.24 - 0.32]	0.19 [0.1 - 0.29]	11.8 [8.4 - 15.2]
LT50 ♀	25.8 [22.6 - 29.0]	25.2 [17.4 - 33.8]	44 [35.7 - 52.6]	0.57 [0.47 - 0.67]	19.5 [16.2 - 22.6]
LT50 ♂	19.6 [16.4 - 22.7]	10.9 [5.9 - 16.5]	35.7 [30.1 - 41.7]	0.3 [0.18 - 0.42]	16.7 [12.7 - 21]

Table 1: Trait means, genetic variance, total phenotypic variance, heritability, and coefficient of genetic variation in titre and mortality following KV infection in the DGRP

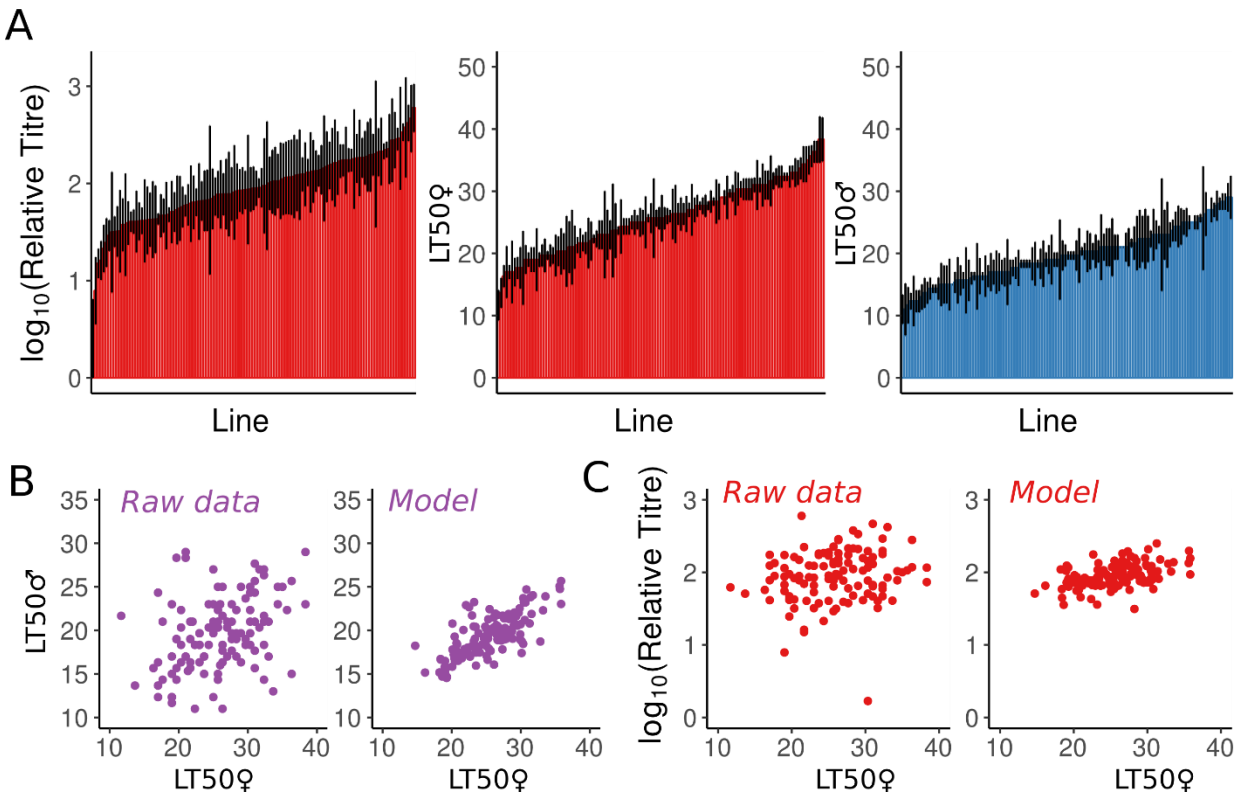

Figure 3: Genetic variation in resistance to KV

(A) We measured LT50 in both sexes, and titre in females, following KV injection in the DGRP. For titre, each bar represents the mean (and standard error) titre relative to fly genome copy-number, as assessed by qPCR for 5 vials of 10 flies for each of DGRP 125 lines. For LT50, each bar represents the mean time until half the flies (in a vial of 10) were dead, for three vials per line, per sex. (B, C) We used a multi-response linear mixed model to calculate genetic correlation between the traits. Shown are the raw data (left), and the estimated line effects (right) after accounting for any injection date and qPCR plate effects, and for estimated variance among lines. Each point is a DGRP line measured for both phenotypes. We find a strong correlation between male and female LT50 values (B). We also observe a weak correlation between titre and LT50 (C).

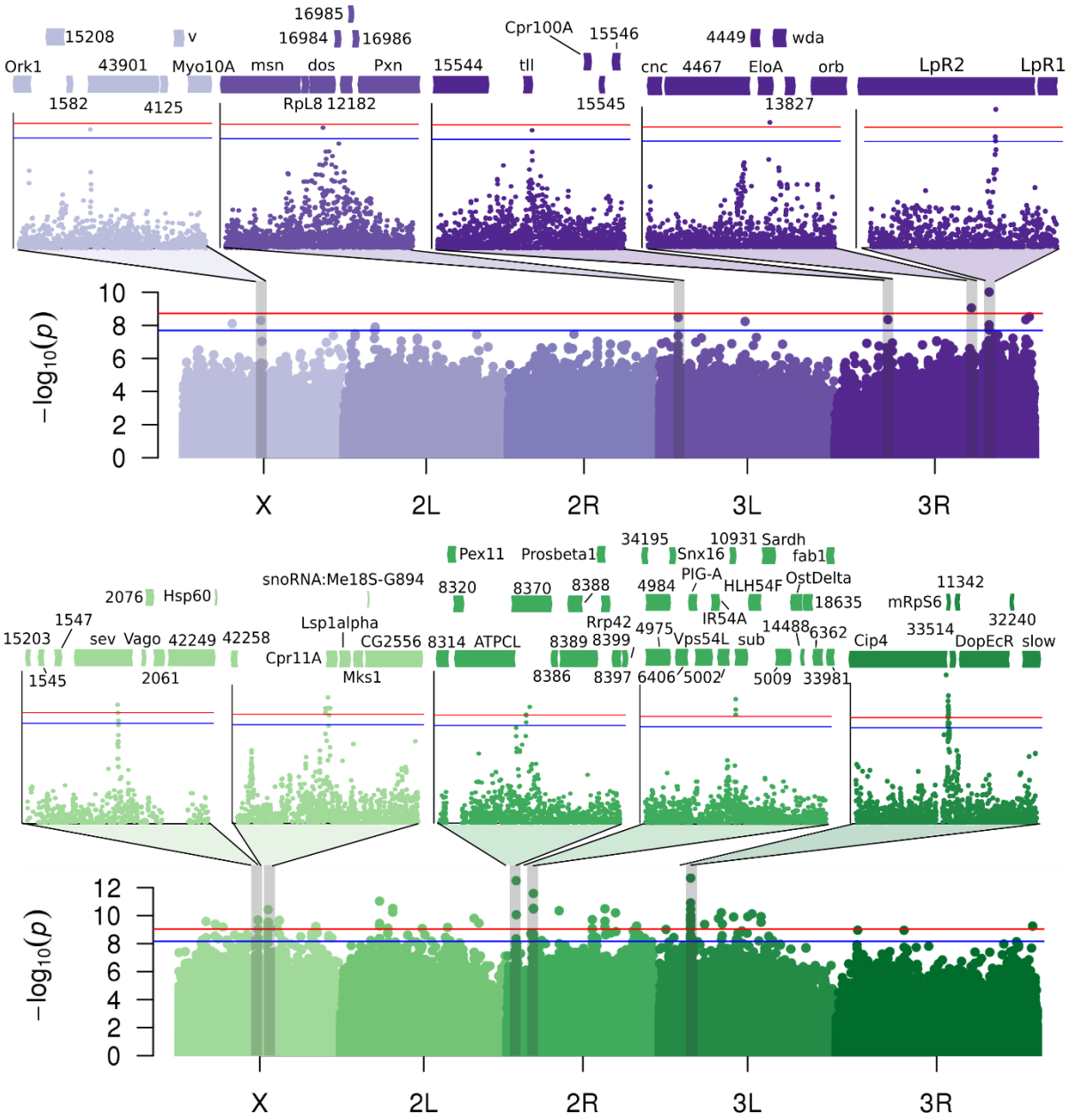

Figure 4: Genome-wide association of polymorphism in the DGRP with KV-induced titre and mortality

Manhattan plots showing the p-value for the effect of each polymorphism on viral titre (purple) and mortality (green). The top SNPs for each phenotype are shown in expanded inset panels, including surrounding genes. “CG” is omitted from gene identifiers due to space constraints. Horizontal lines show significance thresholds obtained through simulation (p_{sim} = 0.05 in blue; p_{sim} = 0.01 in red).

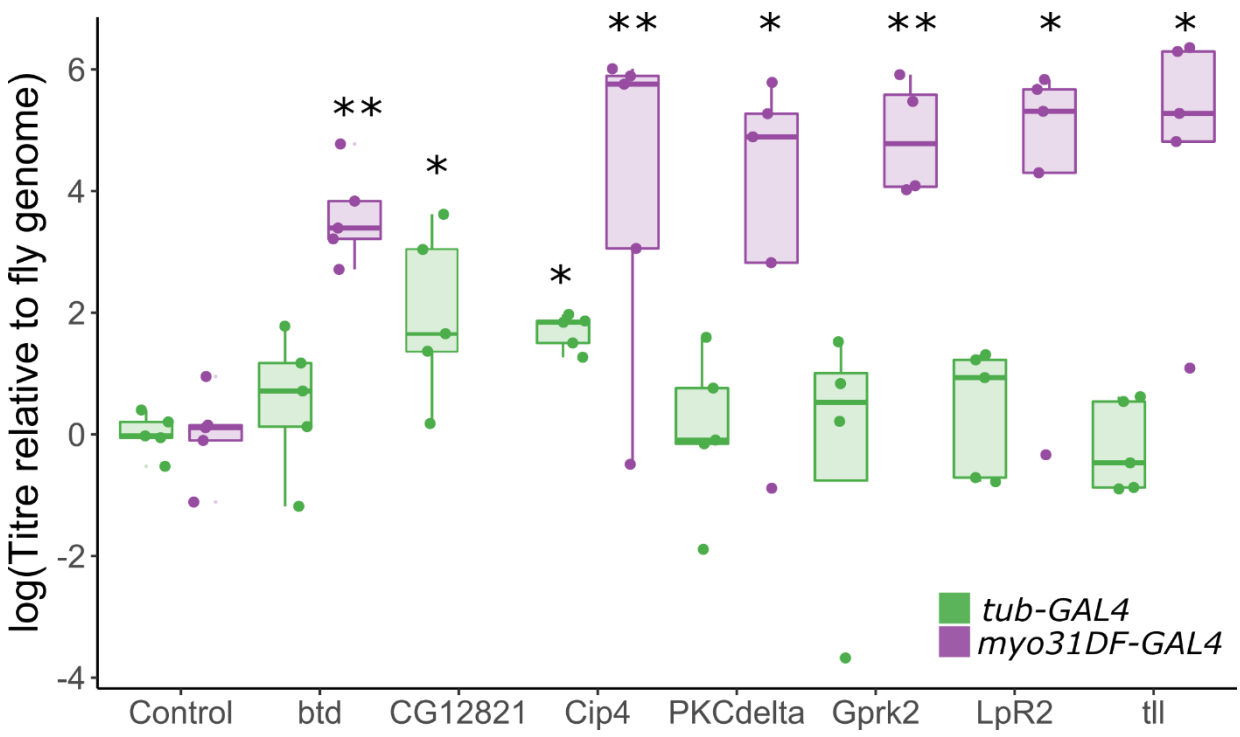

Figure 5: Confirmation of antiviral genes identified in GWAS

KV titre was measured in flies expressing a foldback hairpin targeting 19 genes identified in the GWAS, using GAL4 lines that knock each down in either the whole fly (*tub-GAL4*, green) or specifically in the gut (*myo31DF-GAL4*, purple). Only those causing a significant increase in titre are shown here. (*MCMCp < 0.05; **MCMCp < 0.01)

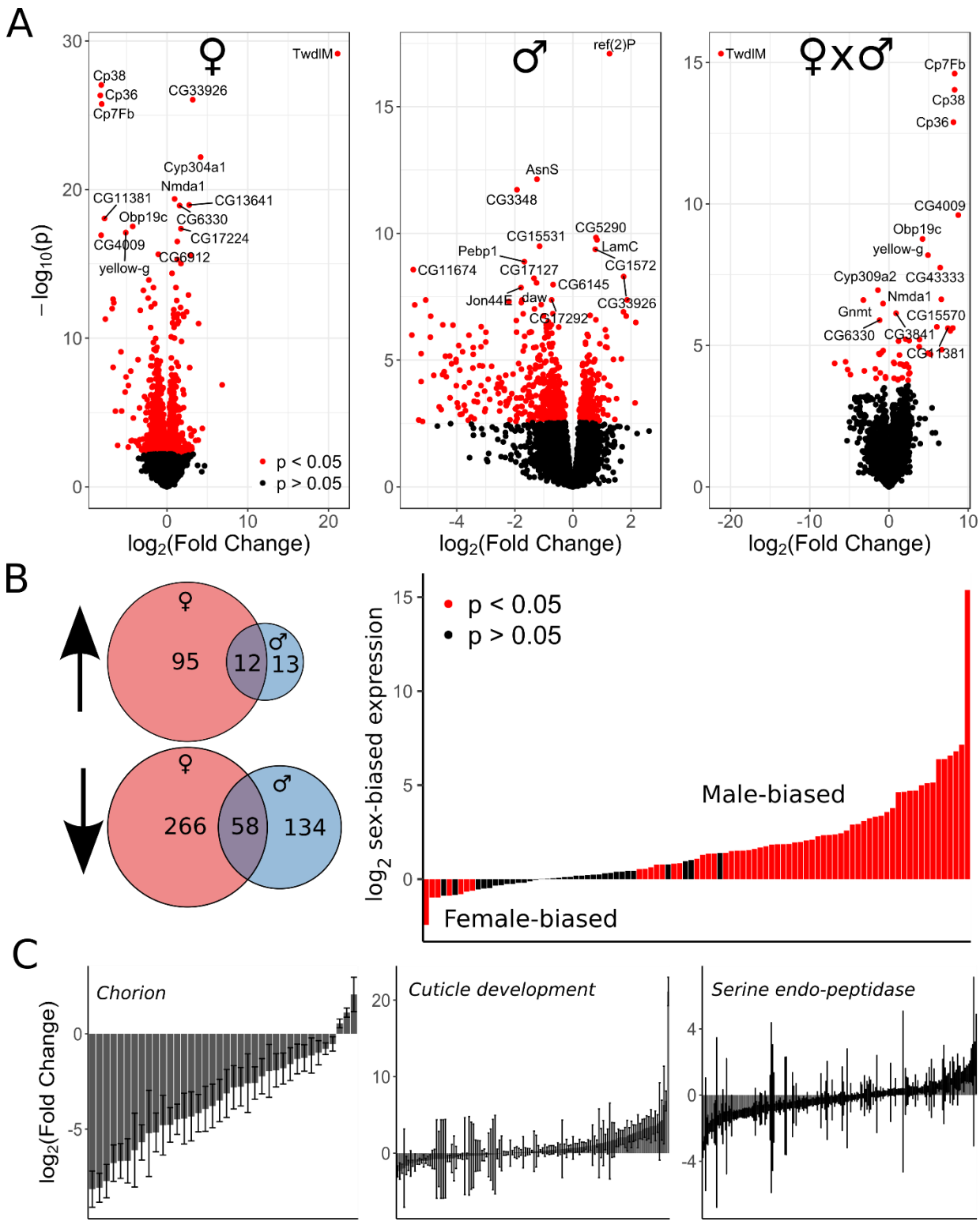

Figure 6: KV induces differential regulation of chorion, cuticle development, serine endopeptidase, and male-biased genes

(A) Volcano plots showing fold changes and p-values from Wald tests for differential expression of *D. melanogaster* genes following KV infection for females (left), males (center), those different between the sexes (right). In each panel, the 15 genes with the smallest p-values are labelled. Many of the genes differentially regulated between the sexes are those highly significant in females. (B) Venn diagrams show genes significantly differentially expressed in response to KV ($p < 0.05$, fold change > 2). Of the 96 genes that were only upregulated in

females, many were already highly expressed in males prior to infection (B, right). Plots show the expression differences between uninfected males and female transcriptomes, in the 96 genes which are specifically upregulated in females and not males. (C) The top GO enrichment terms for each GO class (Molecular Function, Biological Process, Cellular Component) were genes involved the chorion, cuticle development, and serine endopeptidase activity. For each plot, estimated fold changes and their associated standard errors are plotted for every gene in a GO term, regardless of the significance of the Wald test. Generally, chorion genes are downregulated, cuticle development genes are upregulated, and serine endopeptidases are downregulated.

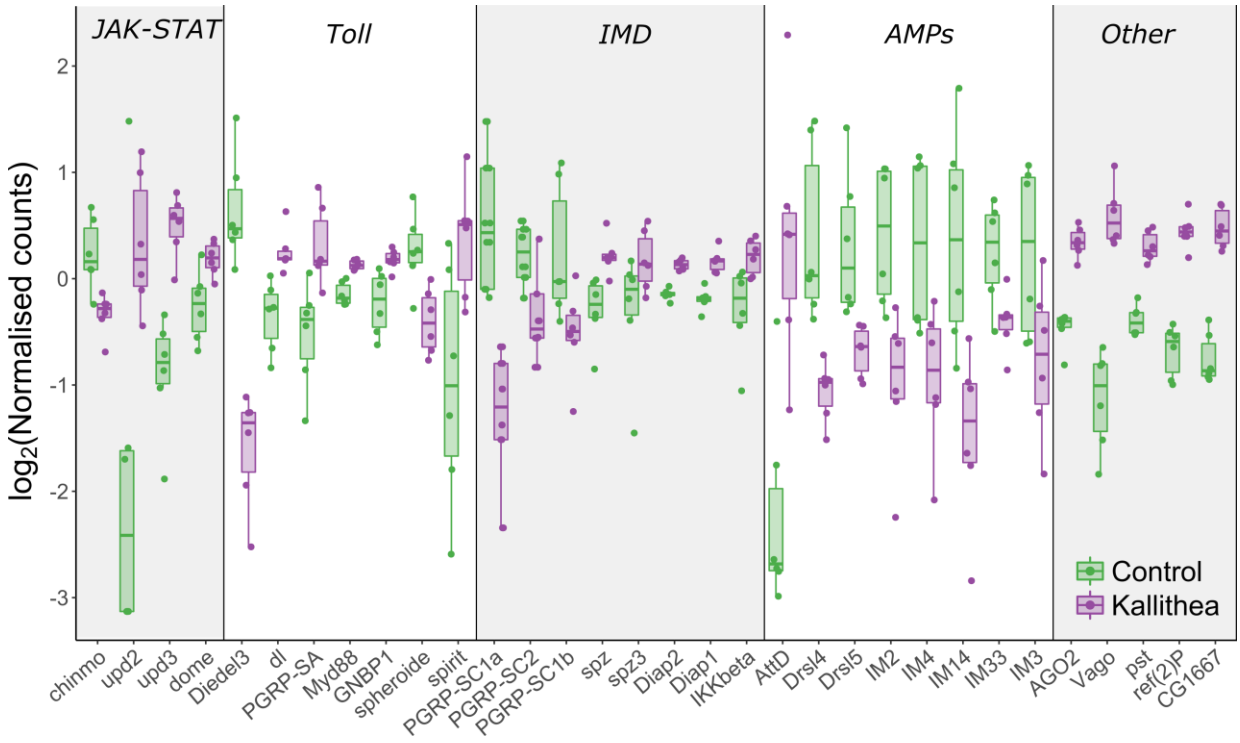

Figure 7: Immune-related genes differentially expressed following KV infection

Read number normalised by library size and by mean expression level for each gene (to facilitate visual comparison) is shown for uninfected flies (green) and KV-infected flies (purple). Each point is the normalised mapped read count for a single gene in a single library. The JAK-STAT, Toll, and IMD pathways appear to be generally upregulated, but canonical downstream NFκB genes, including immune-induced molecule genes and the *Bomamins* (Clemmons et al, 2015), are downregulated. Other genes include antiviral RNAi effector *AGO2*, RNAi cofactor *Vago*, genes identified in previous viral resistance (*pst, ref(2)p*) GWAS, and the STING orthologue *CG1667*.

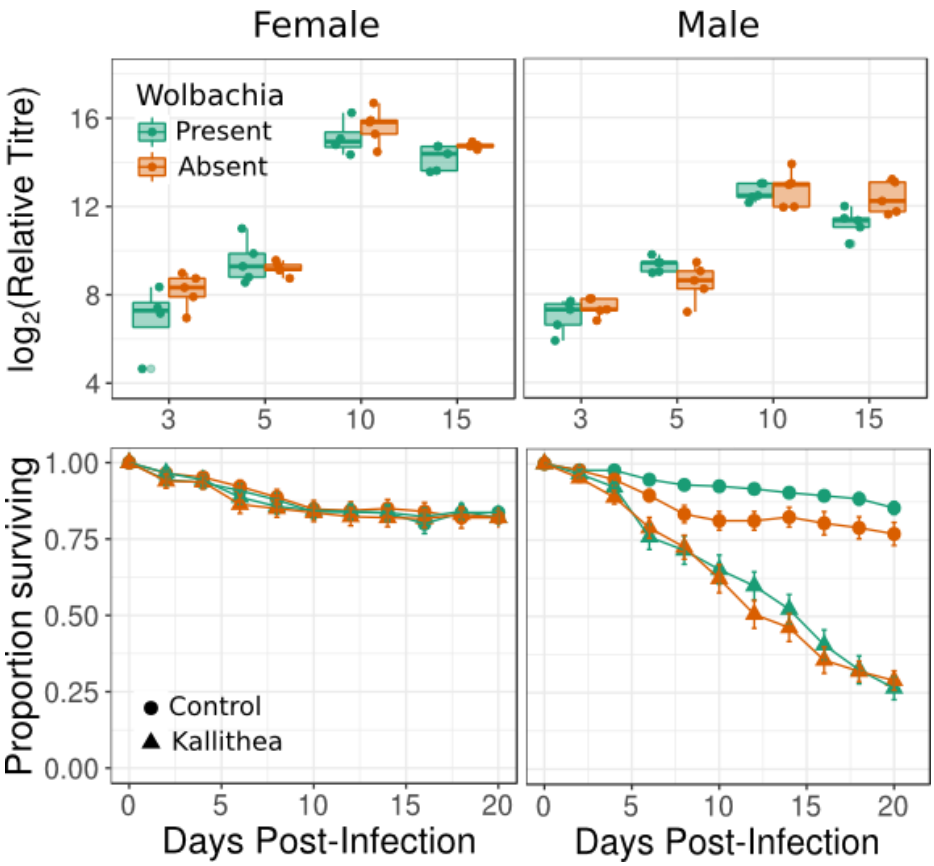

Figure S1: No effect of *Wolbachia* on KV growth or KV-induced mortality

Upper panels: log-transformed relative viral titre in *Wolbachia* positive (green) or negative (orange) *OreR* female and male flies. Lower panels: mortality curves for gradient control-injected (circle) or KV-injected (triangle) *OreR* female and male flies, with or without Wolbachia.

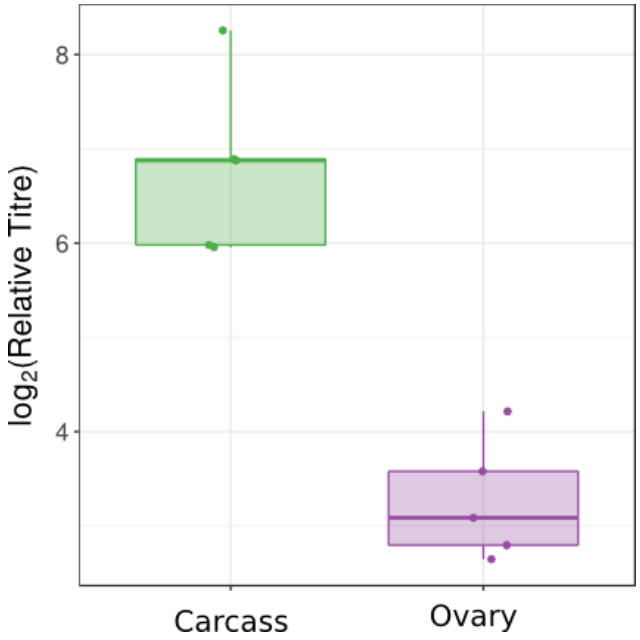

Figure S2: KV enriched in carcass relative to ovary

Females had higher viral titres in non-ovary tissues at 3 DPI. However, this could be affected by the route of infection, and the average ploidy of each sample.

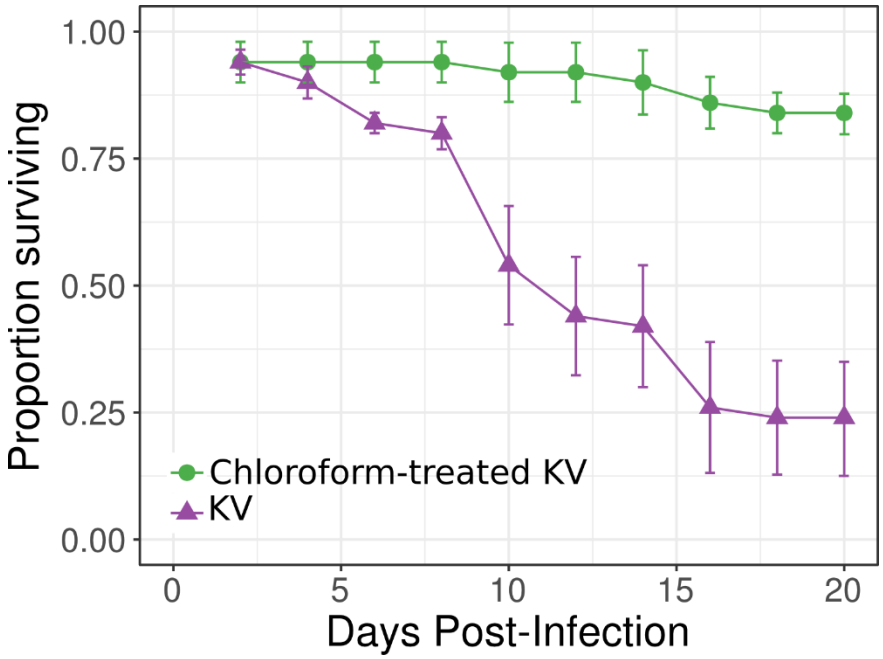

Figure S3: KV-induced male mortality is not caused by contaminating RNA viruses

Chloroform-treatment will inactivate enveloped viruses such as KV, but unenveloped viruses (including most +ssRNA viruses) retain infectivity. We confirmed mortality following KV infection was not caused by contaminating viruses DAV, Nora, or DCV by comparing injection of the KV isolate with (green) or without (purple) inactivating chloroform treatment.

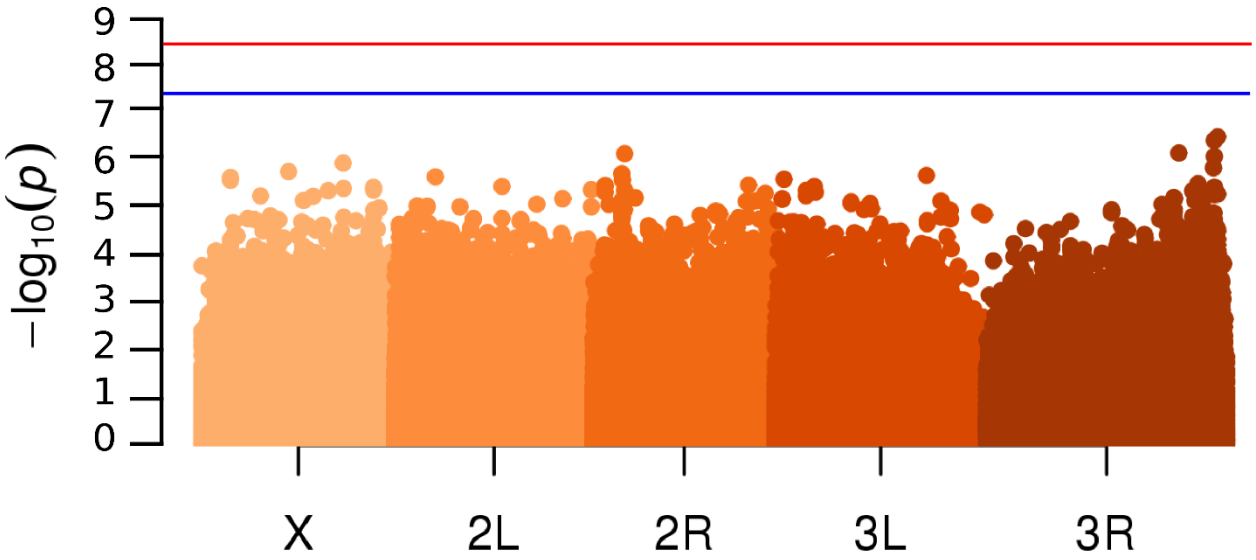

Figure S4: Sex-by-genotype interaction significance manhattan plot

No polymorphism had a significant effect on sex-specific mortality. The blue line denotes p_{sim} = 0.05 and the red line is p_{sim} = 0.01.

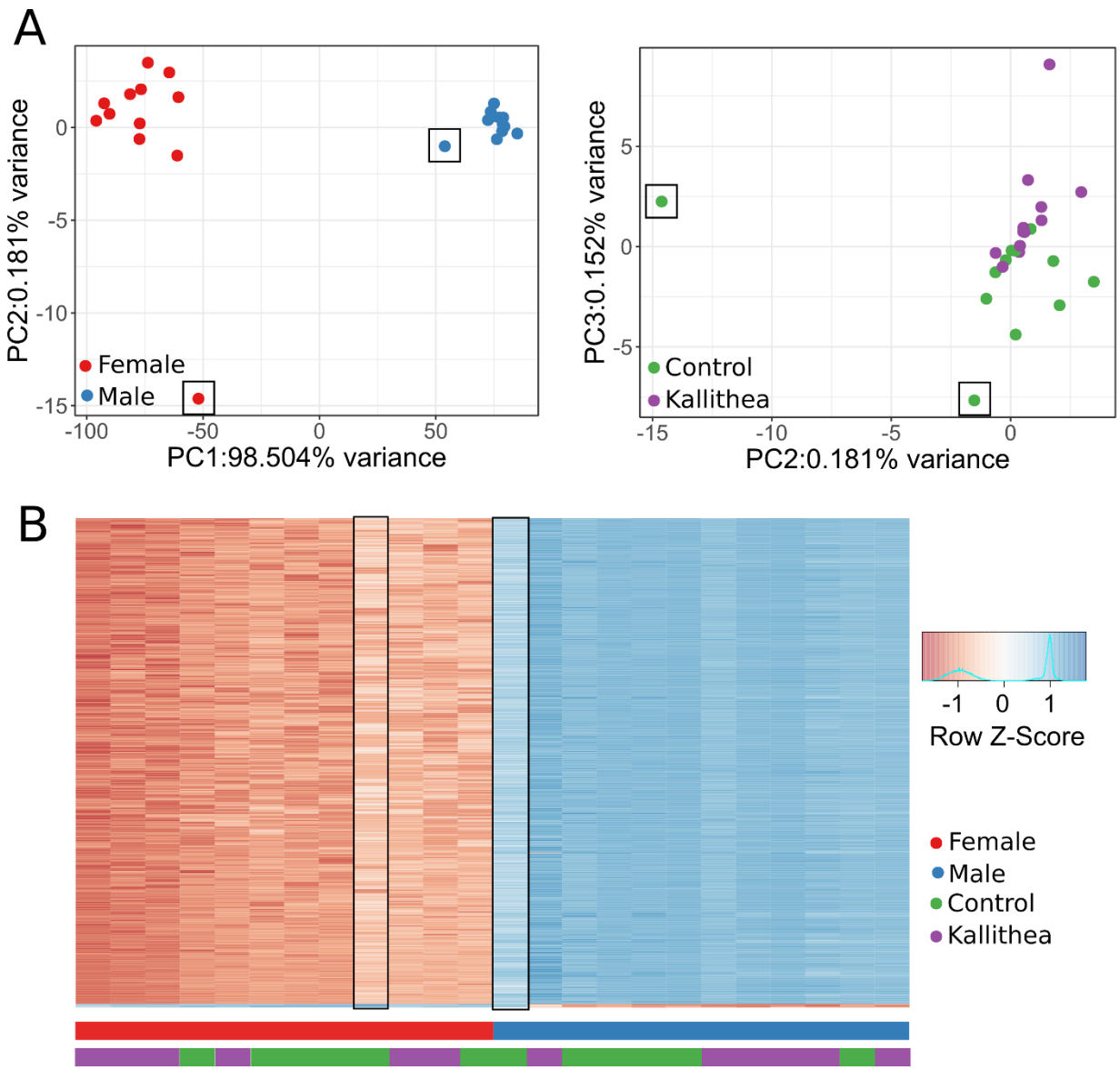

Figure S5: Principal components analysis of read counts per gene in RNA-sequencing data

(A) Each point is a library. Males (blue) and females (red) are separated on PC1. Control-injected (green) and KV-injected (purple) are separated on PC3. For (B), we clustered libraries based on expression of the 1000 most variable genes, where each row on the heatmap is a gene, and the columns are libraries. Together, these analyses identified two possible outlier libraries (black rectangles in A and B). We reran all analyses with these libraries excluded, but found our results remained qualitatively unchanged. The only differences were that *spz* was no longer significantly induced by KV (Figure 6) and that GO enrichment of cuticle development was no longer the highest enriched biological process in the GO term analysis, but was the second (behind outer dynein arm).

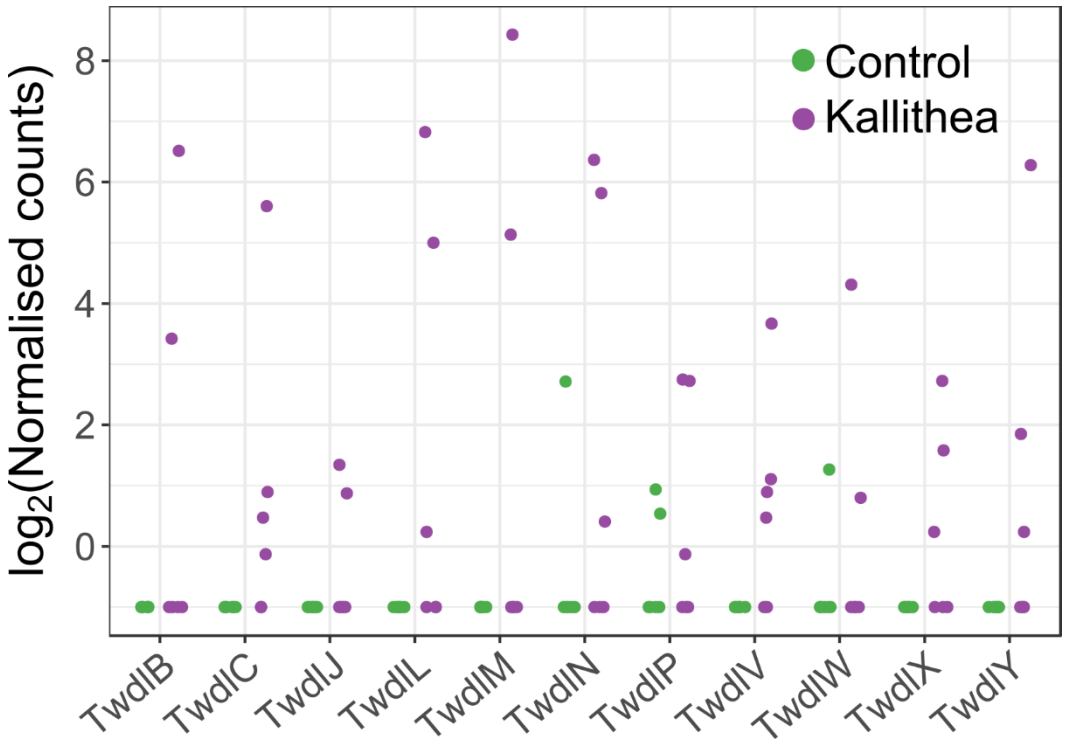

Figure S6: Variable differential expression of the Tweedle gene family

A subset of KV-infected (purple) vials showed very high expression of Tweedle genes, whereas these were mostly unexpressed in control (green) adult flies.

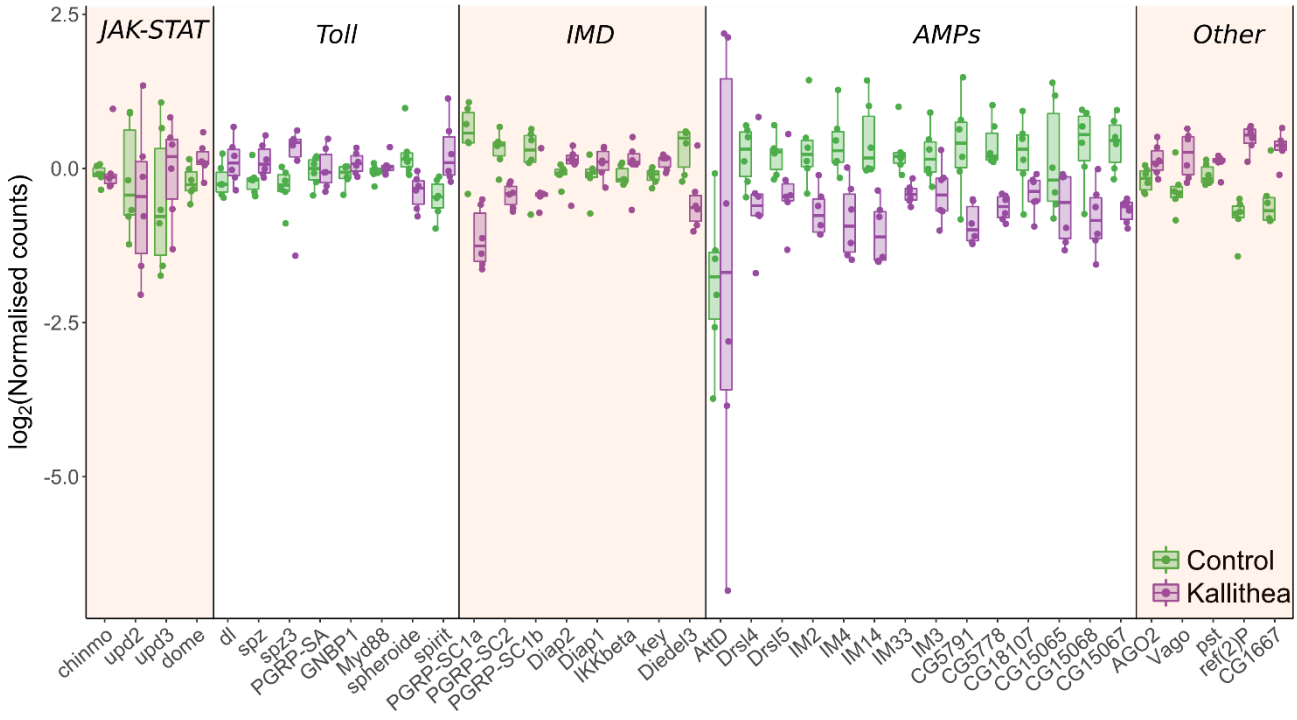

Figure S7 Differential expression of immune-related genes in males

DE of immune genes in males largely mirrored females (Figure 7). IMD, and Toll appear upregulated, with downregulated AMPs. JAK-STAT pathway genes are not convincingly upregulated in males, although these sex-specific differences are not significant.

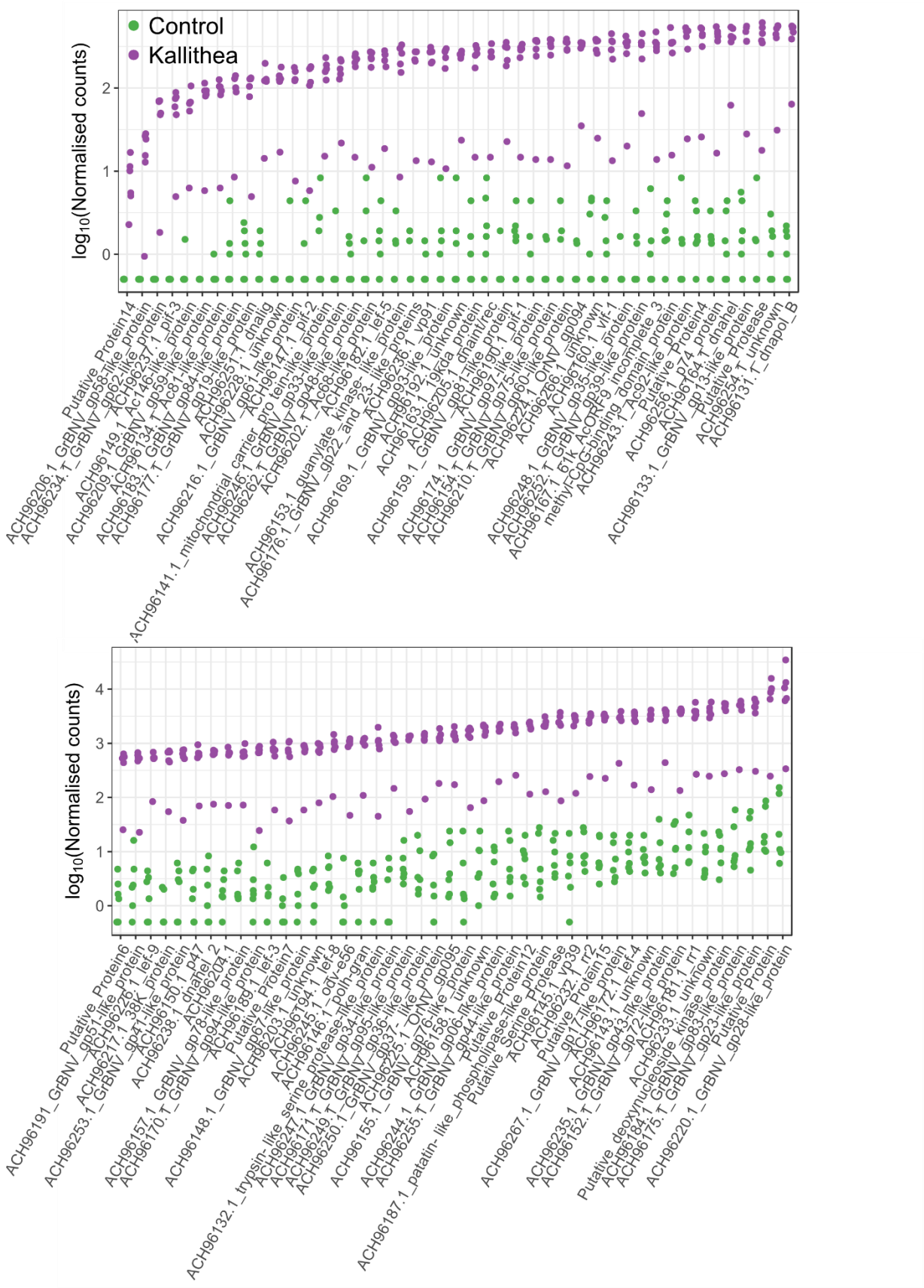

Figure S8: Expression of Kallithea Virus genes

Most KV genes are expressed at 3 DPI. One KV-injected vial of flies had a lower titre infection. Control libraries also showed mapping to KV genes, most likely due to a low level (<0.5%) cross-contamination among libraries run together. The lower panel is a continuation of

the upper panel.

Table S1: Significant GWAS hits

Table S2: Significant GO term enrichment for GWAS hits

Table S3 Differentially expressed genes

Table S4 Significant GO terms for DE genes